Chemical Engineering Journal xxx (2018) xxx-xxx

SAND2018-6200J

Contents lists available at ScienceDirect

Chemical Engineering Journal

journal homepage: www.elsevier.com

Pendant/bridged/mesoporous silsesquioxane nanoparticles: Versatile and biocompatible platforms for smart delivery of therapeutics

Achraf Noureddine[a, *], C. Jeffrey Brinker[a, b, c, *]

[a] Center for Micro-Engineered Materials, University of New Mexico, Albuquerque, NM 87131, USA
[b] Chemical and Biological Engineering, University of New Mexico, Albuquerque, NM 87131, USA
[c] Advanced Materials Laboratory, Sandia National Laboratories, Albuquerque, NM 87123, USA

ARTICLE INFO

Keywords:
Silsesquioxane
Periodic Mesoporous Organosilica
Nanoparticles
Therapeutics
Triggered-release
Synergistic release

ABSTRACT

Silsesquioxane nanoparticles are composed of repetitive organosilica fragments in their frameworks and are now recognized to have outstanding functional fertility. Depending on the organosilane and the synthetic pathways, silsesquioxane NPs can be pendant, bridged, dense or porous. Recently the diverse functionalities of mesoporous silsesquioxane nanoparticles have been exploited for the sake of drug-related biomedicine. Fine-tuning the silsesquioxane nanoparticles characteristics allow not only a superior retention capacity of therapeutics without the need of any further modification, but also a controlled release through various environmentally-stimulated triggers. The main focus of the present review is to highlight the different types of silsesquioxane nanoparticles and their exceptional features focused on controlled delivery of drugs, proteins, antibodies and DNA through pH, redox or light stimuli.

1. Introduction

Currently, we are facing a major problem of delivery of chemotherapeutics into diseased cells. A short half-life of the drugs and their off-target activities requires high dosages to be administered, resulting in significant side-effects to healthy tissues [1]. Recently, nanomedicine has emerged as a means to deliver drugs to tumor area by either active or passive targeting and to deliver their protected payload therein while minimizing side effects. In this field, different systems such as liposomes [2–5], polymers [6–8], polymerosomes [9], silicon nanoparticles [10–14], and hydrogels [15] were used and some formulations are even approved by the American Food and Drug Administration [16] (FDA). However, these systems present several downsides leading to serious barriers to their long-term application *in vivo* such as dose-related toxicity, drug leakage, and stability in biosystems. Siloxane-based (Si–O–Si) nanomaterials, made through sol-gel processes, appear to be one of the most potent candidates to handle that burden because of their biocompatibility (recognized as generally safe by FDA [16,17]), versatile morphologies, controlled pore size and volume (when porous), and surface chemistry; altogether dictating the fate of the nanoparticle and its payload. In the realm of siloxane-based nanoparticles, one must distinguish between two groups:

1.1. Pure and organically-modified mesoporous silica nanoparticles (MSNs and ORMOSIL respectively)

Pure silica SiO_2 MSNs are prepared using a "universal" tetralkoxysilane silica source (e.g. TMOS, TEOS, TPOS), whereas ORMOSILs $(SiO_2)_{1-x}(RSiO_{1.5})_x$ (R = organic group, x = its molar ratio to main silica source) incorporate a minor amount of organosilanes to confer functional surface activity to nanomaterials. This group has been extensively investigated in nanomedical research over the past decade and has been the subject of many recent reviews [18–54]. Therefore we have limited the scope of this review to the following Group:

1.2. Silsesquioxanes: pure organosilica nanoparticles $RSiO_{1.5}$

These are engineered by exclusive use of organosilane(s) through a standard sol-gel process [55–60] (hydrolysis-polycondensation reactions under acidic, basic or nucleophilic (F^-) catalysis). Pendant monosilylated or bridged polysilylated organosilanes can participate in

* Corresponding authors at: Centennial Engineering Center (CEC), Center for Micro-Engineered Materials, The University of New Mexico, Albuquerque, NM 87131, USA.
Email addresses: anoureddine@unm.edu (A. Noureddine); cjbrink@sandia.gov (C.Jeffrey Brinker)

https://doi.org/10.1016/j.cej.2018.01.086
Available online xxx
1385-8947/

Sandia National Laboratories is a multimission laboratory managed and operated by National Technology & Engineering Solutions of Sandia, LLC, a wholly owned subsidiary of Honeywell International Inc., for the U.S. Department of Energy's National Nuclear Security Administration under contract DE-NA0003525.

the formation of pendant or bridged silsesquioxane (herein, designated as PSQ or BSQ respectively) (Scheme 1). Generally, the development of these nanoparticles is more complicated than their silica counterparts because of the extensive participation of organic fragments that can affect the solubility or other physiochemical properties of the precursors. When a mesoporous silsesquioxane framework is obtained upon use of a structure-directing agent (e.g., surfactant), it is also referred to as Periodic Mesoporous Organosilica (PMO) (Scheme 1). Incorporation of a structure-directing agent renders the formation of porous PMO nanoparticles (nanoPMOs) even more difficult than dense PSQ or BSQ nanoparticles; however, scientists have been able to overcome serious synthetic challenges and PMOs have successfully reached the nanoscale [61,62]. In addition to the fact that PMOs incorporate the above-mentioned advantages of MSNs such as tunable pores size and volume, they nonetheless exhibit a fundamental difference compared to MSNs and ORMOSILs, wherein their homogeneous distribution of organic moieties throughout the complete framework makes them unique in terms of functional fertility.

It is worth noting that the nomenclature of different organosilica materials is still a subject of debate, since no clear designation of various frameworks has been established by the IUPAC. For instance, readers can find several papers describing ORMOSILs as PMOs [63–66] or PSQs [67]. Also nanoPMOs can be designated as MON (Mesoporous Organosilica Nanoparticles with analogy to MSNs) [68]. Undoubtedly, the (bio)chemical versatility of PSQ, BSQ and PMO nanomaterials will be their trebuchet into a central part of nanomedical research in the next years. In the next sections we will present a brief evolution of the history of silsesquioxane materials and describe how they have been used to date in nano-medicine as drug/biomolecule delivery vehicles.

In the present review we focus in particular upon the controlled release properties of silsesquioxane nanoparticles. Only nanomaterials made solely by organosilane(s) and exhibiting a drug release behavior will be reviewed, namely PSQ, BSQ and PMO nanoparticles (although one example showing PMO-like nanoparticles possessing an extremely high organosilane extent is reported for biocompatibility studies).

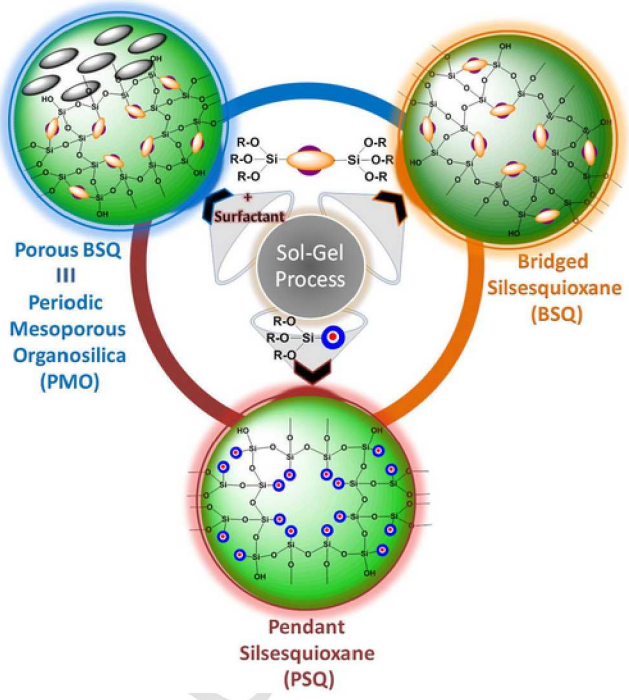

Scheme 1. Representation of the classes of sol-gel processed silsesquioxanes: pendant monosilylated organosilanes produce PSQ, bridged polysilylated organosilanes yield BSQ, bridged polysilylated organosilanes in the presence of surface-directing agents yield PMO.

2. A strand of history

After the revolutionary concept of periodic micro/mesoporous silica materials was introduced in 1990–1992 by Kato et al. [69] and Kresge et al. [70,71], pioneering studies of silsesquioxane materials began in 1999–2000 with the work of Inagaki [72] and Ozin [73], who reported the first PMOs with ethane (–Si–C_2H_4–Si–) bridged fragments, prepared using a base-catalyzed aqueous (hydrolytic) route, and Stein who produced ethylene (–Si–C_2H_2–Si–) bridged PMOs with subsequent functionalization (*via* bromination) [74]. Paving the way toward applications in medicine, Brinker et al. used an aerosol assisted evaporation-induced self-assembly process [75,76] to produce the first PMO nanoparticles incorporating aliphatic (–Si–$(CH_3)_n$–Si–, n = 2,3,6,8,10), unsaturated (–Si–CH_3–C_2H_2–CH_3–Si–) or aromatic (–Si–C_6H_4–Si–) bridging organosilanes [77]. Shea et al. reported more detailed studies of the sol-gel synthesis of monolithic bridged silsesquioxane aerogels and xerogels using 15 different alkane-, alkene-, alkyne-, aromatic-, functionalized- and organometallic-bridged precursors [78] and investigated thereafter the mechanism of gelation [79]. The self-assembly/nanostructuring mechanisms of BSQ were fundamentally studied [80–89] and since then the engineering of new bridged silsesquioxane materials has been a very fertile ground for catalysis [90–101], light harvesting [94,102–106], luminescence [102,107–112], tailoring the hydrophobic/hydrophilic balance [113], metal sequestration/stabilization [114–117], thin films [102,105,107,110,118–120], reactivity-probes [121–123], molecular sieves [124–127], structure-direction [73,128–136] or related relevant fundamental studies [133–158].

3. Compatibility with biosystems

Biocompatibility is a fundamental requirement of any nanosystem intended for biomedical applications. At a minimum nanoparticle carriers should show minimal cellular toxicity, as judged e.g. by dose-dependent toxicity assays and potential to cause hemolysis of red blood cells. It is further imperative that the nanoparticle carriers exhibit *in vivo* stability so as to avoid aggregation and reduce non-specific binding and uptake by the mononuclear phagocyte system (MPS) and thereby increase circulation times and enhance both passive and active targeting

3.1. Synthesis

Following the first report of the synthesis mesoporous silsesquioxane nanoparticles via an aerosol EISA process by Brinker and coworkers [77] in 1999, many following works developed PSQ and BSQ nanoparticles through a hydrolytic sol-gel (Fig. 1a) process using a plethora of mono-,bi- or polysilylated organosilanes with pendant or bridging organic groups ranging from simple aliphatic to polyaromatic, metal-chelating and highly functional fragments. The morphologies (Fig. 1b-i) can be tailored so that nanospheres [159–165], nanocrystals [166], hollow nanospheres [61,167–171], nanodonuts [172], nanotubes [125,173–176], nanorods [177,178], multipodal PMOs [179], deformable hollow PMOs [180], and core-shell nanoparticles [181–185] were produced via soft or hard templating pathways with size ranging from a few to several hundreds of nanometers. The synthesis strategies of PSQ, BSQ and PMOs nanoparticles are comprehensively reviewed in some excellent papers [68,186,187].

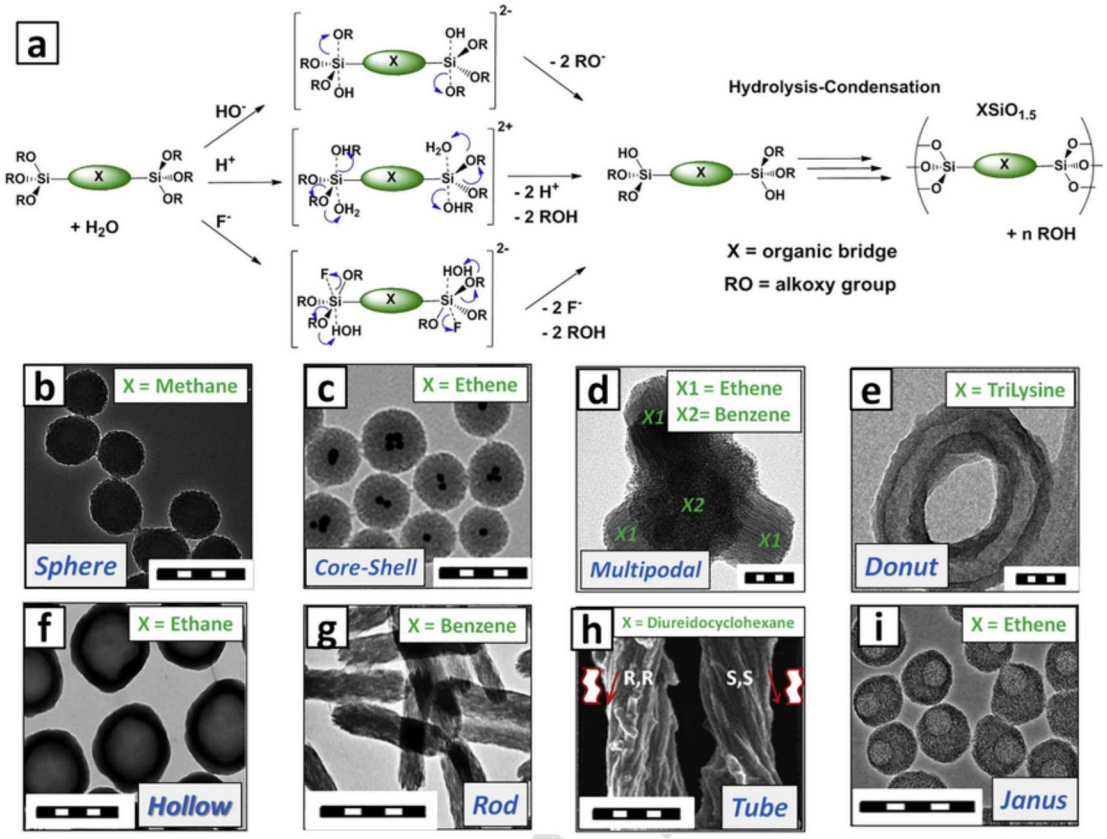

Fig. 1. General mechanisms of hydrolytic sol-gel process via basis, acidic, or nucleophilic catalysis (a) and b-i) electron microscopy images of different morphologies obtained for silsesquioxane nanoparticles. Scale bars (b-e) = 100 nm and (f-i) = 500 nm. b) Reproduced with permission. [1] Copyright 2012, Royal Society of Chemistry. c) Reproduced with permission from [2]. Copyright (2014) American Chemical Society d) Reproduced with permission. [3] Copyright 2015, Wiley-VCH e) Reproduced with permission. [4] Copyright 2016, Wiley-VCH f) Reproduced with permission. [5] Copyright, 2016, Elsevier. g) Reproduced permission [6] Copyright 2017, Wiley-VCH. h) Adapted with permission from [7]. Copyright (2001) American Chemical Society i) Reproduced with permission from [8]. Copyright (2015) American Chemical Society.

3.2. *In vitro cell viability and in vivo biodistribution*

Biocompatibility is an important criterion for biomedical applications and it has been demonstrated for pendant and bridged silsesquioxane nanoparticles in several studies.

In pioneering work, the Prasad group showed in 2003 that 20–25 nm vinyl-amine PSQ nanoparticles used as carriers for a hydrophobic photosensitizing anticancer drug, are non-invasive for UCI-107 and HeLa cell lines [188]. In 2010, the same group used the same PSQ (in a PEGylated form, labeled with DY776 and radionucleus ^{124}) to study their *in vivo* biodistribution and clearance [67]. It was shown that 360 h post-injection, the majority of nanoparticles were cleared through hepatobiliary excretion (Fig. 2c, d). After 15 days of exposure, selected organs from dissected mice showed no histological abnormal behavior or toxicity (Fig. 2a, b). They concluded that this system is "potentially an ideal attribute for use as biocompatible probe for *in vivo* imaging". More recent work [32,189] on dense BSQ made purely by trypsin-cleavable oxamide bridges [190] (Fig. 2e,f) or by mixing thioether [191] with porphyrin or a two-photon sensitizer showed complete biocompatibility. Additionally, bridging porphyrin/iodine BSQs used for wide-field photodynamic/photothermal therapy also showed high *in vivo* compatibility [192].

Switching to PMOs, Huo et al. described a straightforward synthesis of nanoPMOs with different bridging groups (methylene, ethylene, ethenylene and phenylene) [193]. Importantly, they showed that FITC-labeled methylene-PMOs have a high biocompatibility demonstrated by HeLa cell viability of >75% even at high nanoparticle concentrations (125 μg/mL media) after 24 h exposures at 37 °C (Fig. 3a). Furthermore, ethenylene and bispropyldisulfide mixed PMOs were synthesized with different extents of the bridging organosilanes [194]. These nanomaterials beautifully showed a degradation behavior triggered by mercaptoethanol simulating the reducing conditions in the cancer cell. Again, these PMOs showed a very good biocompatibility towards MCF-7 cells where less than 20% cells died after 3 days of incubation at high concentration reaching 125 μg/mL (Fig. 3b). More recently, phenylene-bridged PMOs were produced in different morphologies (wires, rods, bent rods and spheres) simply by tuning the co-solvent during the synthesis (Fig. 3c), and their compatibility towards HeLa cells was studied [195]. It was shown that less cell death occurred as the morphology is extended and this was attributed to easier internalization in the case of sphere-like morphology (Fig. 3d). Overall PMOs with different organic bridging groups in different studies showed biocompatible behavior promising their increasing use in nanomedicine.

3.3. *Hemolytic activity*

Red blood cell (RBC)-friendly behavior is a further criterion for nanosystems to be considered for clinical translation.

The very first reliable studies of hemolytic activity were carried out by the Kuroda and Takeoka groups where they proved that ethenylene-bridged colloidal PMOs nanoparticles (20 nm) showed less hemolytic activity than analogous MSN and dense silica nanoparticles towards bovine RBC [196] (Fig. 4a). In fact, it has been suggested that the hemolytic activity of siliceous materials is related to the presence and density of silanol groups on the surface of the material [30,197,198],

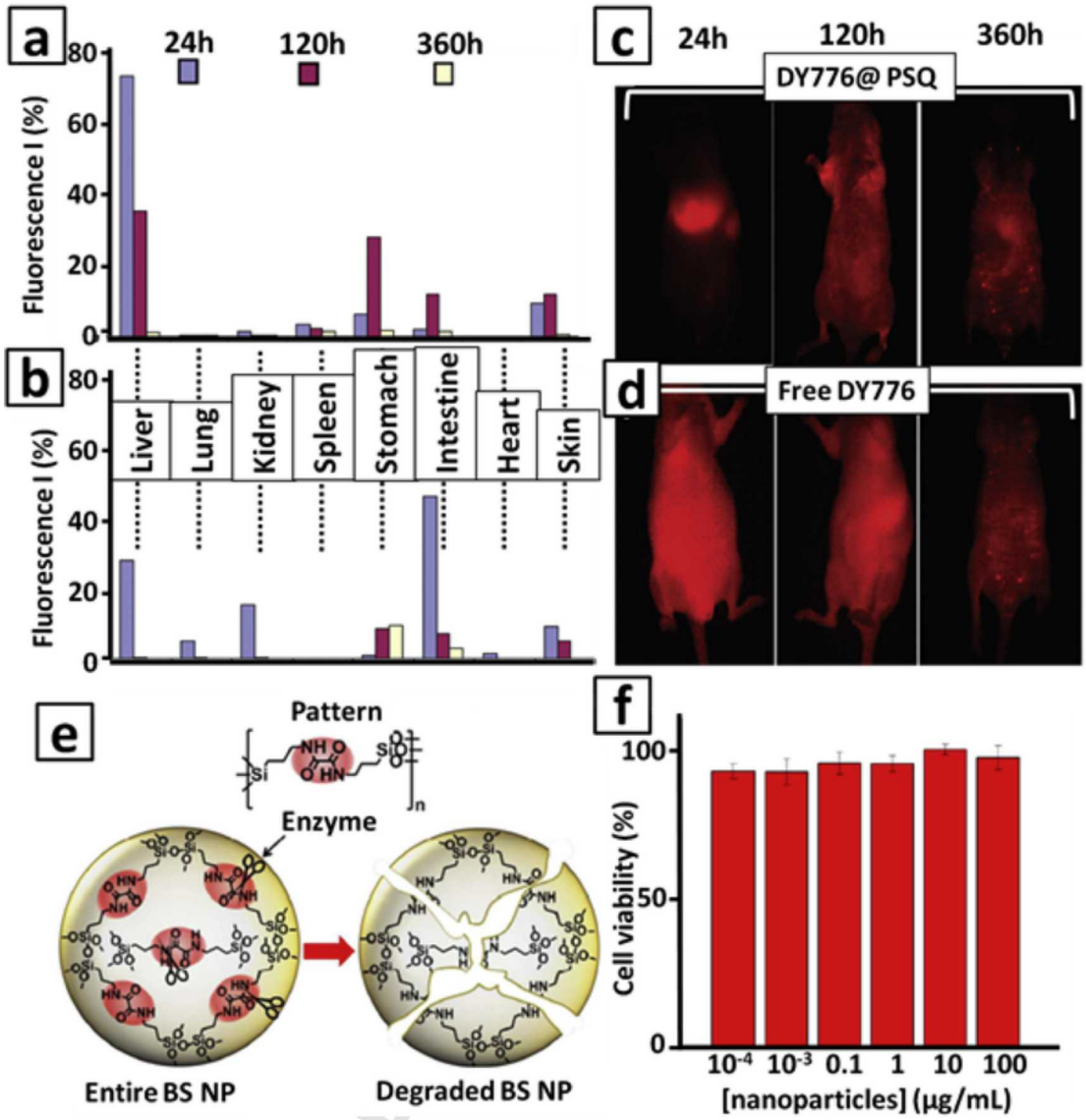

Fig. 2. Quantitative estimation of fluorescence acquired from various organs of mice injected with (a) DY776 PSQ and (b) free DY776, at 24, 120, and 360 h; (c) Clearance of the DY776 PSQ injected intravenously into the mice and (d) a comparison with the free DY776 injected mice as control. The same acquisition time was maintained for all the time points of imaging. e) Schematic representation of the enzymatic degradation of BSQ via the cleavage of amide bonds by trypsin. f) Cell cytotoxicity of HeLa cells incubated with BSQ for 24 h. a-d) Adapted with permission from [9]. Copyright (2010) American Chemical society. e,f) adapted with permission [10]. Copyright (2015), Royal Society of Chemistry.

and more precisely, to the electrostatic interaction between negatively charged silanolates and positive head groups of the RBC membrane lipids [198]. The lower hemolysis induced by PMOs is explained mainly by the lower density of silanol groups on the surface due to the high extent of organic bridging groups, but also, by the lower acidity of the existing silanols due to high concentration of electron-donating ethenylene groups [55].

Later on, phenylene PMOs showed better compatibility to RBC than their MSN counterparts [199] (Fig. 4c,d). This result was demonstrated in parallel to an important *in vivo* behavior of these nanoparticles, where intravenously injected mice dosed with 100 mg/kg for 2 months showed no death or uncommon behavior as the exposed organs confirmed an excellent histocompatibility for the studied nanomaterials. Also, triple hybridized yolk-shell PMO-like MSNs (containing up to a 75% organosilane mix: methylene, thioether and phenylene) were proven to have very low toxicity toward breast cancer MCF-7cells even at 1200 μg/mL and negligible hemolytic activity (< 2%) even at concentrations as high as 2000 μg/mL [200] (Fig. 4b).

Unlike MSNs where passivation of the surface by organic moieties (e.g., PEG) is crucial to overcome or reduce the hemolytic activity [201], PMOs are now proven to have a low hemolytic potential even without any subsequent modification.

3.4. Colloidal stability and targeting properties

The high extent of organic fragments within a silsesquioxane framework reduces correspondingly the silanol concentration which has a direct effect on the charge and the stability of this family of nanomaterials. For pure silica nanoparticles, which are moderately to strongly negatively charged at neutral pH depending on their extent of porosity, the charge repulsion responsible for the colloidal stability of nanomaterials is reduced in high ionic strength physiological media inducing the aggregation of administered nanoparticles. Another barrier for nanoparticles to be translated into nanomedicine is the mononuclear phagocytic system (MPS), which is the first line of defense against the "foreign invaders" inhibiting their intended therapeutic efficiency. A potential solution is the passivation of the outer surface by "stealthy"

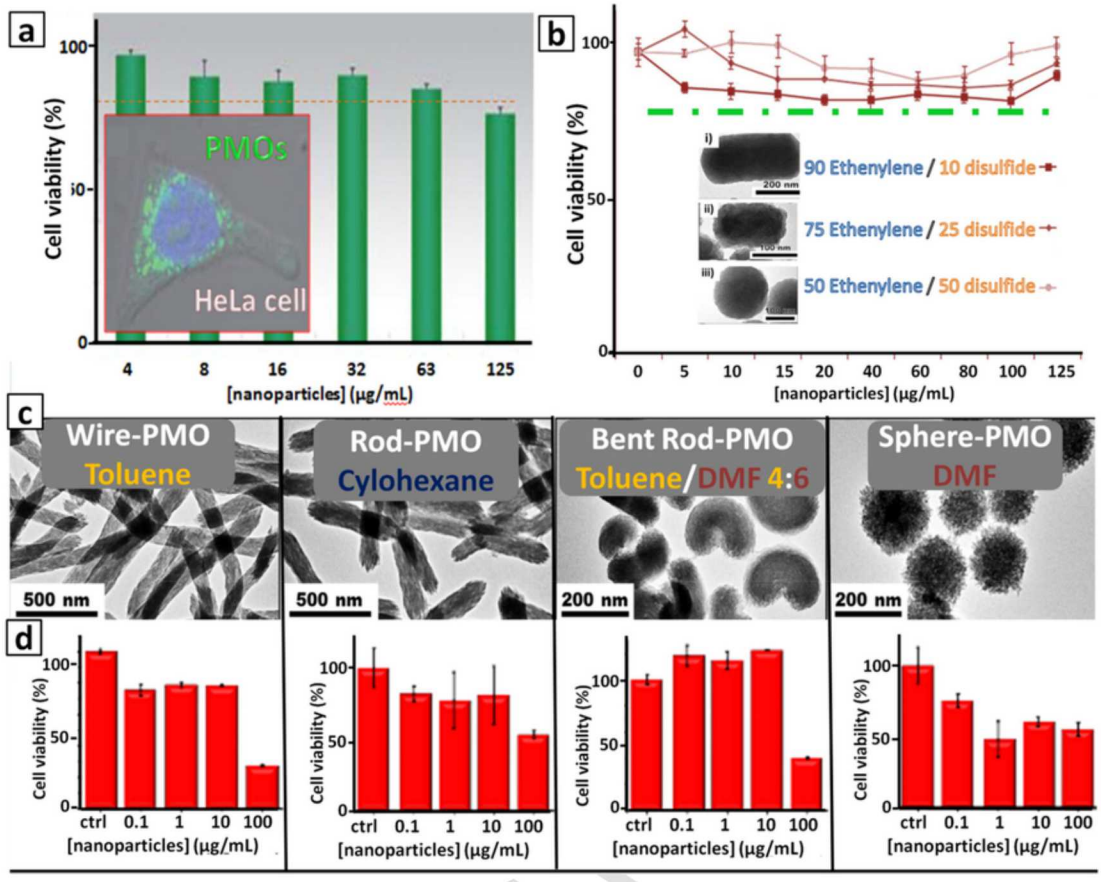

Fig. 3. a) Dose dependent toxicity of methylene-bridged PMO nanoparticles exposed to HeLa cells for 24 h at 37 °C. The inset shows FITC-PMOs internalized in the cytoplasm of HeLa cells. b) Dose dependent toxicity of ethylene/disulfide PMO NPs exposed to MCF-7 cancer cells after 72 h of incubation. The enclosed TEM images show the effect of the organosilane mixture on the morphology of the PMOs. adapted from [11] c) Evolution of morphology of phenylene-bridged PMO NPs with variation of the organic cosolvent(s) in the reaction media d) Dose dependent toxicity of PMOs exposed to HeLa cells for 24 h at 37 °C. a) Adapted with permission [1]. Copyright (2012), Royal Society of Chemistry b) adapted with permission [11]. Copyright 2014, Wiley-VCH. c,d) Adapted with permission [6] Copyright 2017, Wiley-VCH.

PEG that reduces protein adsorption (opsonization) and uptake by the MPS, thereby increasing the circulation time of nanoparticles. In contrast to MSNs where numerous papers treated this aspect [201–206], very few works have outlined the colloidal stability of pure organosilica nanomaterials, as they are still considered "new to the market". Della Roca et al. post-functionalized Pt-BSQ (developed in Section 4.2.1) with PEG through an EDC chemistry to increase its *in vivo* performance. They have also successfully conjugated onto the BSQ nanoparticles targeting ligands for $\alpha_v\beta_3$ integrin and sigma receptors, respectively, cyclic Arginine-Glycine-Aspartate (cRGD) and anisamide (via a PEG spacer). The additional value of the targeting ligands was highlighted *in vitro* and *in vivo*. In the former case, IC_{50} values were reduced 2–10 times for DLD-1 and HT-29 colon and BxPC-3 pancreatic cancers when cRGD was anchored and 3.5 times for AsPC-1 pancreatic cells with PEG-anisamide introduced as the targeting molecule. In addition, *in vivo* performance was confirmed in the latter case by the reduction of AsPC-1 tumor volume in female athymic nude mice by 50% and 40% respectively for PEG- or PEG-anisamide-bearing BSQ compared to untreated control mice. The targeting effect of anisamide on H460 and A549 lung cancer cells was also highlighted by the same group using gadolinium-based BSQ nanoparticles where the (60–70%) reduced amount of released Gd on solely PEGylated BSQ (compared to native non-PEGylated Gd-BSQ) was corrected and even enhanced after conjugation with targeting anisamide (130–140%). The low Gd release from untargeted PEGylated BSQ is an expected result of the low cell uptake induced by the PEG stealth behavior.

Lu and Zhao [180] recently reported novel deformable hollow tetrasulfide-PMOs passivated by maleimide-PEG and exhibiting excellent dispersibility in cell culture media. Although the system was not compared to non-PEGylated PMOs, we expect the latter to be unstable in physiologically relevant media.

Overall the passivation of PMOs by moieties that increase their stability in bio-relevant environments is crucial for their bioapplications. Targeting will enhance the therapeutic effect of administered nanosystems and increase their potential for *in vivo* translation.

3.5. Comparison with MSNs

Although a library of silsesquioxane nanoparticles of different morphologies was presented here, their synthesis remains highly challenging compared to MSNs especially if the goal is to yield a full batch of monosized and homogeneously porous nanoparticles. As a rule, synthesis becomes more difficult and complicated as the organic bridges get larger or more voluminous since the organic moieties may exhibit a preferential interaction or difficult solubilization.

In terms of biocompatibility, organosilica may be considered at least as biocompatible as silica nanoparticles. Silica is generally recognized as safe by the FDA as it dissolves overtime to yield non-toxic silicic acid. On the other hand, the possibility to insert degradable fragments in a silsesquioxane framework also allows its degradation with rates potentially exceeding those of native MSNs and with the potential of triggered degradation. Additionally, on the hemocompatibility level, silsesquioxanes exhibit a lower hemolytic potential due to their lower

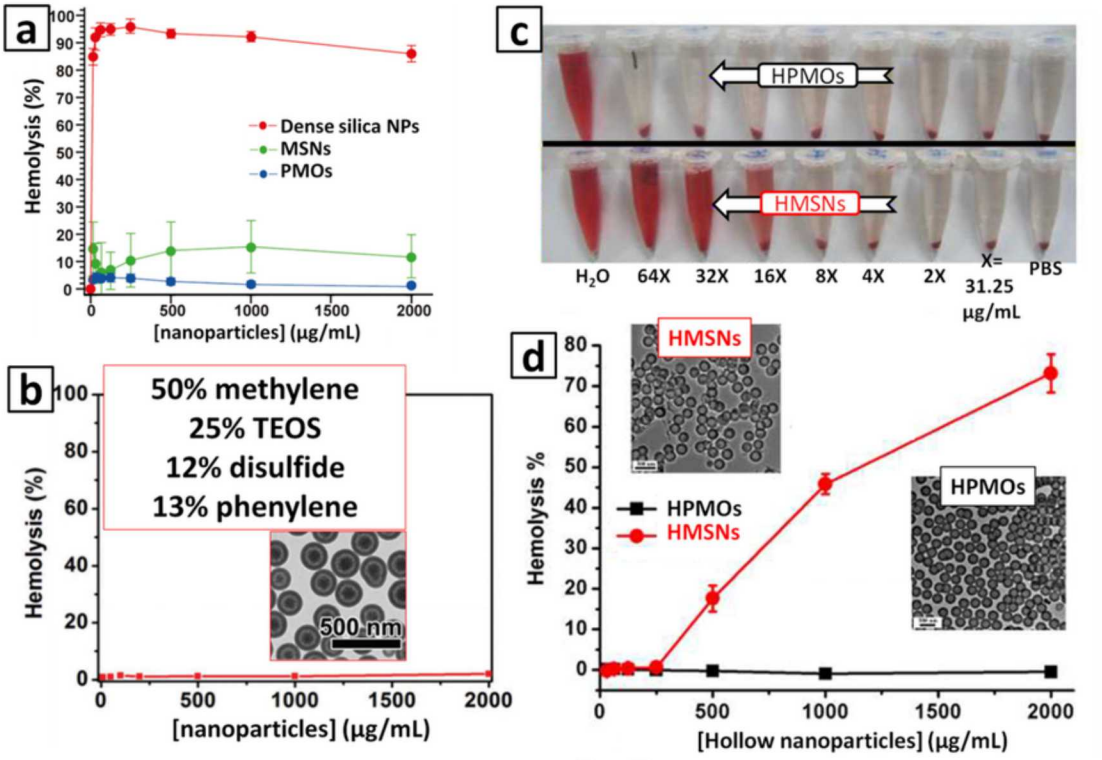

Fig. 4. a) Hemolytic activity of dense silica (red), mesoporous silica (green) and ethylene-bridged periodic mesoporous organosilica (blue) nanoparticles in different concentrations. b) Percentage of hemolysis of RBCs incubated with the yolk–shell-structured triple-hybridized PMO nanoparticles at different concentrations. The inset in (b) is an electron micrograph of the utilized nanoparticles along with their composition. c) Digital photos showing hemolytic effects after 2 h co-incubation with HPMOs and HMSNs. Water was used as the positive control and PBS as the negative control. Colloidal NPs were suspended in different concentrations to interact with RBCs; d) Percentage of RBC hemolysis after co-incubation with HPMOs and HMSNs at different concentrations ranging from X = 31.25 to 64X = 2000 μg/mL (n = 3, inset: TEM images of HPMOs and HMSNs, scale bars: 500 nm) a) Adapted with permission from [12]. Copyright (2011) American Chemical society b) adapted with permission [13]. Copyright 2014, Wiley-VCH. c,d) adapted with permission [14]. Copyright 2014, Wiley-VCH. (For interpretation of the references to colour in this figure legend, the reader is referred to the web version of this article.)

silanol concentration, which is a major determinant of hemolysis. As an example hollow PMOs showed no hemolysis whereas hollow MSNs should up to 75% hemolysis at 2 mg/mL, (Fig. 4d).

The colloidal stability of organosilica and silica nanomaterials is excellent in water when the pH is much greater or lower than the pKa. Due to electron providing effects of organic fragments, the pKa of silsesquioxanes is shifted toward neutral pH ($pKa_{silsesquioxane} \sim 5–7$) compared to pure silica MSNs ($pKa_{MSN} \sim 1.5–3$). This would suggest that MSNs have a greater stability under neutral conditions. In both cases, however, when exposed to salt-rich media the nanoparticles will physically aggregate as a function of time, requiring surface passivation with PEG or other polymers or supported lipid bilayers for biomedical applications.

4. Stimulus-induced cargo release

Organosilica nanoparticles are being increasingly used in cancer therapy [35,207,208]. The cancer microenvironment is substantially different than that of normal cells and tissues; the acidic and reducing conditions associated with cancer microenvironments have been exploited by researchers resulting in pH- and redox-responsive materials capable of stimulus-triggered release of therapeutics.

4.1. pH-triggered release

The acidic environment of endosomes and lysosomes is a mandatory checkpoint for nanoparticles having undergone endocytosis, and will definitely modify the surface characteristics of the nanosystems (especially the charge). Highly functionalized and drug-laden nanocomposites can then be created in a way to harness this feature for a superior retention through electrostatic attraction or pH-controlled release *via* charge repulsion.

In 2005, Prasad et al. reported an unprecedented work on pendant silsesquioxane (PSQ) NPs for loading and delivery of DNA through a non-viral pathway [209,210]. Aminated and porphyrin-containing positively-charged PSQs were produced to bind negatively charged DNA with an intercalating fluorophore. Gel electrophoresis confirmed the protection of PSQ-bound DNA from enzymatic digestion. The porphyrin and the DNA's fluorophores were the FRET donor and acceptor in order to monitor the proximity (binding) of DNA to the PSQ. Under *in vivo* conditions, a FRET signal decrease implied a separation between DNA and the porphyrin-PSQ framework. This indicated the release of DNA due to the increased acidic conditions in the living cells that induced destabilization of the DNA-PSQ complex. Active DNA delivery to the cell nuclei was evidenced by a pEGFP signal [209]. No PSQ-induced toxicity was observed even up to one month after transfection. This concept was also exploited to achieve *in vivo* gene delivery to the mouse brain [210].

A key example worth reporting even though nanoparticulate systems were not developed: BSQs were obtained using a triazine-bridged bisilylated organosilane exhibiting 3 sites to strongly H-bond cyanuric acid [211] or a prodrug containing three 5-Fluorouracil moieties [212] (Fig. 5). A mild acidic treatment (pH = 5.5) suppresses the H-bonding with the cyanuric acid or prodrug inducing its release and resulting in, good performance on MCF-7 cells. Although these H-bonded molecules are key-fragments of the material skeleton, their release did not induce any structural collapse, establishing these BSQ as promising and reliable frameworks for pH-sensitive drug delivery.

The first application of PMOs in drug delivery was reported in 2013 where hollow PMOs (HPMOs) were prepared by etching a SiO_2 core of

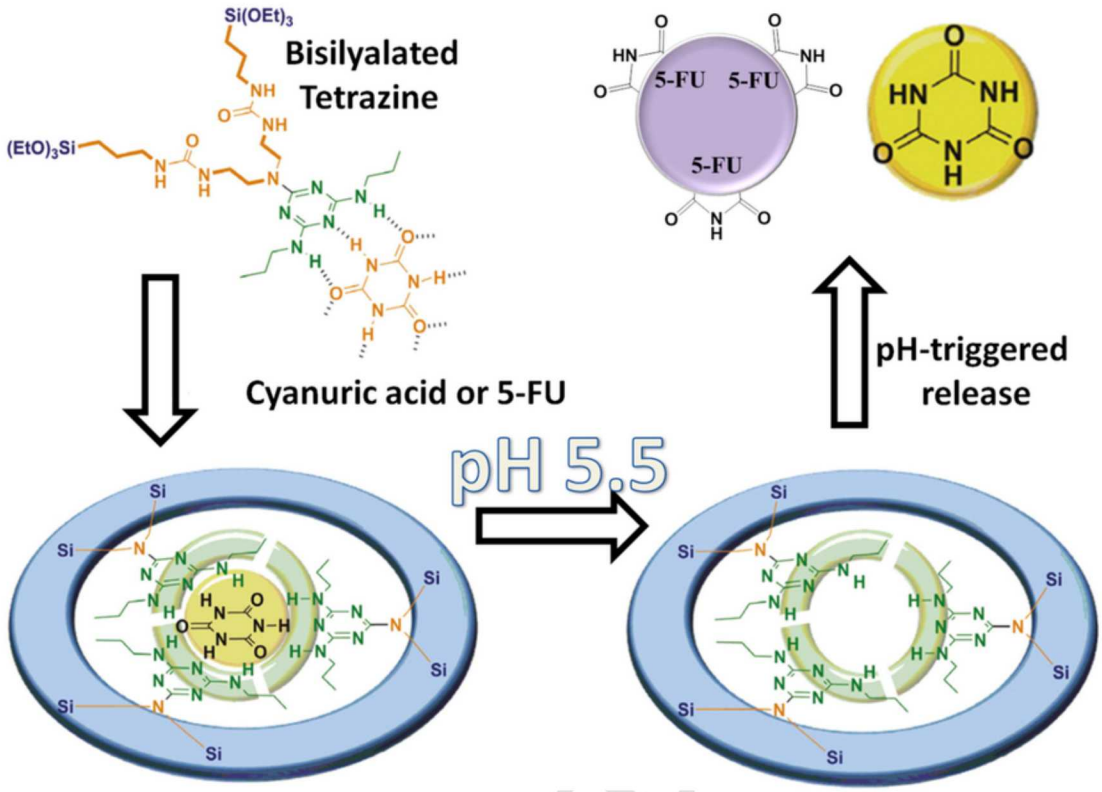

Fig. 5. Representation of the preparation of cyanuric acid or 5-FU loaded pH-responsive BSQ. Upon exposure to acidic conditions, the loaded entity is released after suppression of H-bonds responsible for interaction with the payload. Adapted with permission from [15]. Copyright (2011) American Chemical society.

a core-shell construct [168] (Fig. 6a). First, bulk silica nanoparticles were made according to the Stöber method using TEOS then coated with ethane-, ethylene- or phenylene-bridged organosilanes through a sol-gel process. Based on the difference in condensation degrees [213], the etching procedure was carried out by reacting HF over the silica core for one hour to yield hollow organosilica nanoparticles. Different amounts of HF yielded different etching extents and thus various nanoparticles morphologies, namely yolk-shell (partial etching) and hollow (complete etching) (Fig. 6b, c). PMOs, owing to their hydrophobic character, were then able to efficiently load silibinin, a hydrophobic drug presenting very poor bioavailability [214]. Invasiveness of MDA-MB-231 cells (their capacity of migration and infiltration to neighboring tissues) was assessed *in vitro* upon exposure to free silibinin and loaded and unloaded HPMOs (Fig. 6d). The invasiveness of silibinin-laden HPMOs was the lowest with about only 10% versus 30% for unloaded HPMOs. Free silibinin had no effect due to its hydrophobic character that induced low bioavailability. Hence, the importance of delivery of hydrophobic anti-metastatic drug into cancer cells through a PMO protecting carrier was thus clearly highlighted.

Later on, the same group extended this strategy to make benzene-based hollow organosilica nanoparticles for pH-responsive drug (DOX) and gene (P-gp shRNA) co-delivery to MCH-7/ADR cancer cells [215]. The delivery of genes can restore the sensitivity of accompanying drugs by overcoming the drug efflux pump and therefore allow reduced drug dosages and eventual corresponding side effects.

With a myriad of existing organic groups used in various applications, the production of structured and porous BSQ is far from being a trivial task because of the extensive physicochemical input of organic moieties. The recent advances in nanomedicine require delivery of larger cargoes (proteins, DNA, enzymes, etc.) to the target cell. However, it is highly challenging to apply the common pore swelling procedures used for silica [26,26,216–230] on silsesquioxanes to produce large pore BSQ. Here a unique example stands out [231]. Recently, based on a biphase reaction reported to produce large-pore dendritic MSN [232], a phenylene-bridged silsesquioxane was produced with dendritic pores with sizes 4.6 nm or 7.6 nm depending on the organic phase formulation (Fig. 7a, b). With these unique pore morphologies, they loaded up to 80 μg/mg and 154 μg/mg, respectively, of the protein RNase with a hydrodynamic diameter of 4.7 nm. A sustained release was obtained with the larger pores, where 50% after 10 h and 80% after 72 h were released, whereas 90% release was recorded at 10 h for the smaller pores (Fig. 7c). In this latter case, the size of the RNAse is equal to the average pore size so a preferential adsorption on the external surface was the origin of this fast release of protein. Accordingly, these large pore mesoporous organosilica nanoparticles were applied to MCF-7 breast cancer cells, the results (Fig. 7d) show no effect on cells when they were exposed to free protein whereas the cell viability decreases for 4.6 nm pore particles to 65% with negligible difference between 1, 2 and 3 days since the greatest drug release occurred in the first 12 h. However, the cell viability shows a sustained decrease from 60% to 45% and 32% at one, two and three days, respectively. This result is in accordance with the sustained release profile. This important cell death was attributed to the high amount of RNAse loaded in the pores of these organosilica nanoparticles due to the intrinsic aromatic benzene group of the BSQ framework.

4.2. Redox-triggered release

As silica frameworks have proven to spontaneously degrade via siloxane bond hydrolysis in aqueous systems, they have been extensively applied to biosystems [24,25,33,35–37,57,64,66,204,229,233–240] after Coradin's group reported the introduction of disulfide bridges in dense silica nanoparticles for the first time [241]. However, with silsesquioxanes, the story is different. Ethylene-bridged PMOs of

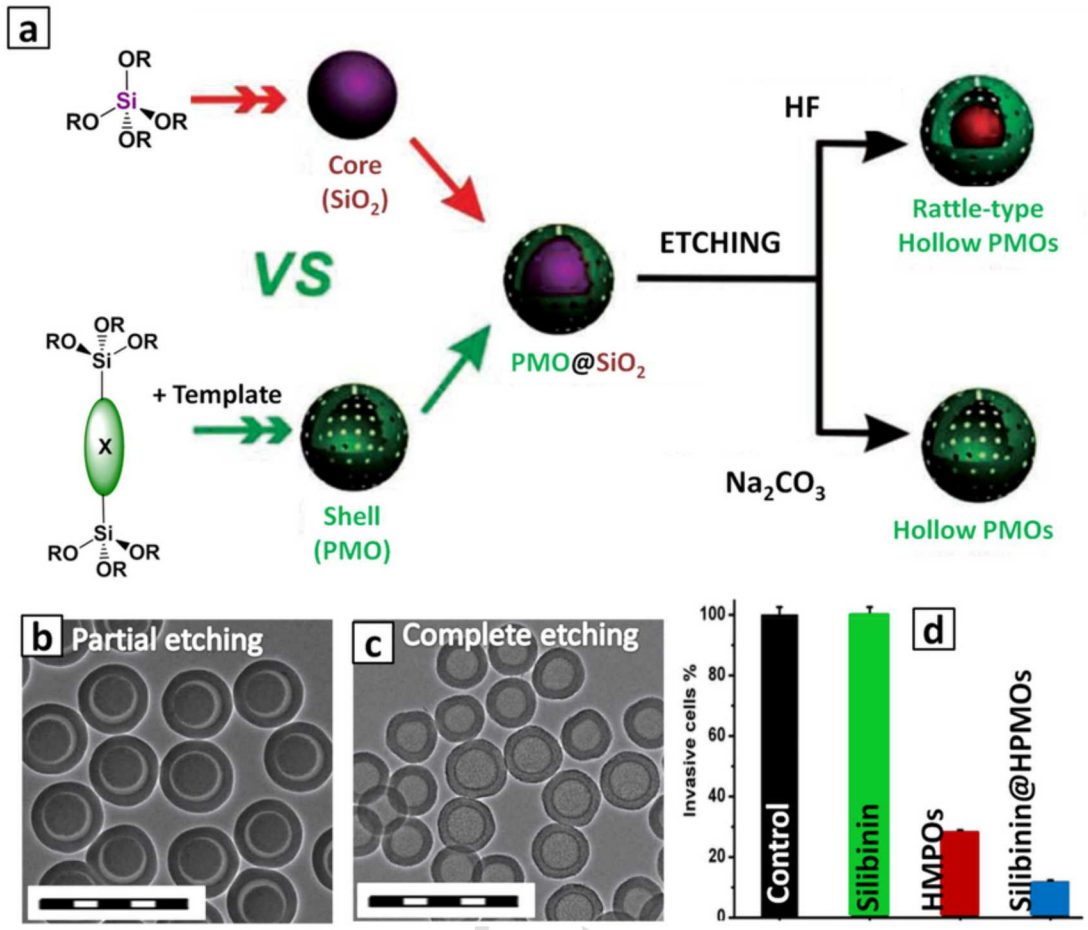

Fig. 6. a) Schematic illustration of the creation of core-shell PMOs@SiO_2 nanoparticles and their subsequent etching pathways to obtain hollow or rattle-type PMOs. X moieties within the framework are representative of phenyl-, ethyl- or ethylene-groups. TEM image of b) yolk-shell (125 μL HF) and c) entirely hollow PMO NPs (500 μL HF), scale bar = 500 nm. d) The percentages of invasive cells ([silibinin] = 20 μg/mL) determined by the invasion assays. Adapted with permission [14]. Copyright 2013, Wiley-VCH.

20 nm and MSN counterparts showed drastically different dissolution behavior in PBS. While up to 85% of MSN were degraded in a week, less than 10% PMOs were dissolved in 2 weeks [196] (Fig. 8a). The degradation mechanism of silica starts occurring on the outer surface by progressive hydrolysis of siloxane bonds resulting in the formation of non-toxic silicic acid $Si(OH)_4$ byproducts, where the rate of dissolution is dominated by the silanol/silanonate concentration on the surface [242]. Also, the degradation behavior highly depends on intrinsic (porosity, condensation degree, surface chemistry) and external (media, nanoparticles concentration) factors. However, organosilica presents a significantly lower silanol content as well as an important participation of organic groups, often hydrophobic, minimizing the effective interface with the water and significantly decreasing the degradation rate. This behavior was confirmed again in ethane-coumarin PMOs [243] (Fig. 8b) where exposure to simulated body fluid (SBF) for 28 days showed no significant effect on the structure of the materials. Small-Angle X-ray Scattering (SAXS) confirmed maintenance of the framework structure and TEM showed no collapse in the morphology (Fig. 8c-d). The mechanisms of degradation of organosilica materials are provided in an excellent review by the Khashab group [242].

This structural stability of organosilica to biological media can be finger-printed by the scientific community due the accumulation and persistence of inert organosilica species in organs. Nevertheless, the functional fertility of organosilica has enabled new frameworks to be created that degrade under biologically relevant conditions. Biologically triggered release is achieved by inserting biologically-cleavable moieties in the organosilica skeleton. Disulfide [168,191,244,245]- and aminoacid-based [190,246] bridged organosilanes were integrated in nanoparticles and resulted in excellent degradation behavior upon redox or enzymatic conditions. The integration of such functions in the organosilica nanoparticles will pave the way into the development of highly biocompatible systems and improved *in vivo* reliability.

4.2.1. Redox-triggered degradability of silsesquioxane matrix for assisted-release

A novel platinum-based BSQ for targeted and controlled delivery of chemotherapeutics to colon and pancreas tumors stimulated by a redox trigger was reported by the group of Lin [247,248]. A synthetic bisilylated molecule bearing a cisplatin or cisplatin derivative (oxaliplatin) was used to make BSQ nanoparticles with Pt^{IV} distributed throughout the framework. Under normal physiological conditions, the Pt^{IV} complex is stable (Fig. 9a) and no or negligible release of cisplatin or oxaliplatin was detected. Upon exposure to the highly reducing conditions of the cancer environment (i.e. L-cysteine, glutathione), Pt^{IV} is reduced to active Pt^{II} and is no more chelated by the surrounding carboxylic groups, thus inducing the release of the cisplatin without requiring particle degradation (Fig. 9b). The Pt^{II} therapeutic effect originates from its capability to intercalate into the DNA strands of targeted cells thus stopping tumor growth. In order to render the reported system more adapted for bioapplications, the external surface was passivated with PEG moieties and, interestingly, it was shown to be slightly less efficient *in vitro* (A549 and H460 lung cancer cells) than the free cisplatin (most probably due the slower cell uptake because of the PEG). However, the *in vivo* efficacy was evaluated on mice bearing A549 and

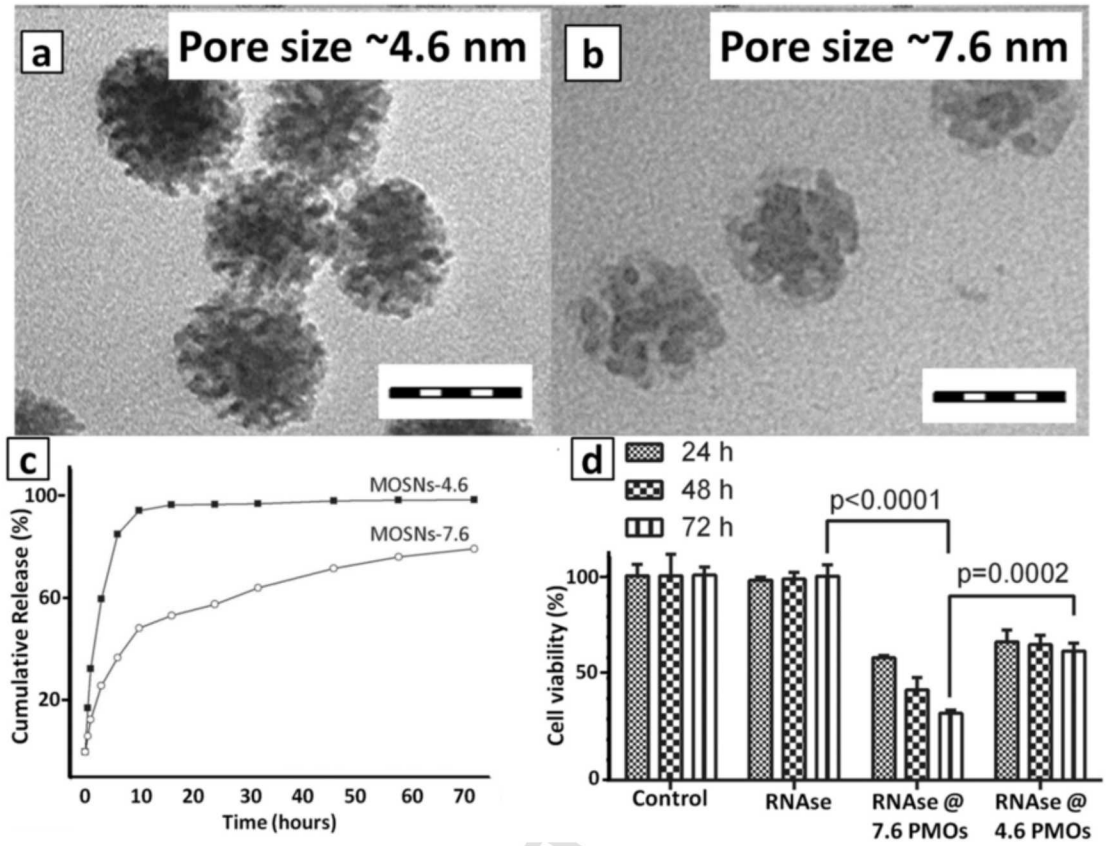

Fig. 7. TEM images showing the difference of electron density between BTSB-based nanoparticles with a) 4.6 or b) 7.6 nm pore sizes, scale bar = 50 nm. c) The RNAse A cumulative release profile of MOSNs-4.6 and MOSNs-7.6 in PBS solution as a function of time. d) Evaluation of RNase A (4 μg/mL) delivery using MOSNs-4.6 and MOSNs-7.6 in MCF-7 cell line after 24, 48, and 72 h via a cytotoxicity assay. Data are presented as mean ± SD. Adapted with permission [16]. Copyright 2015, Wiley-VCH.

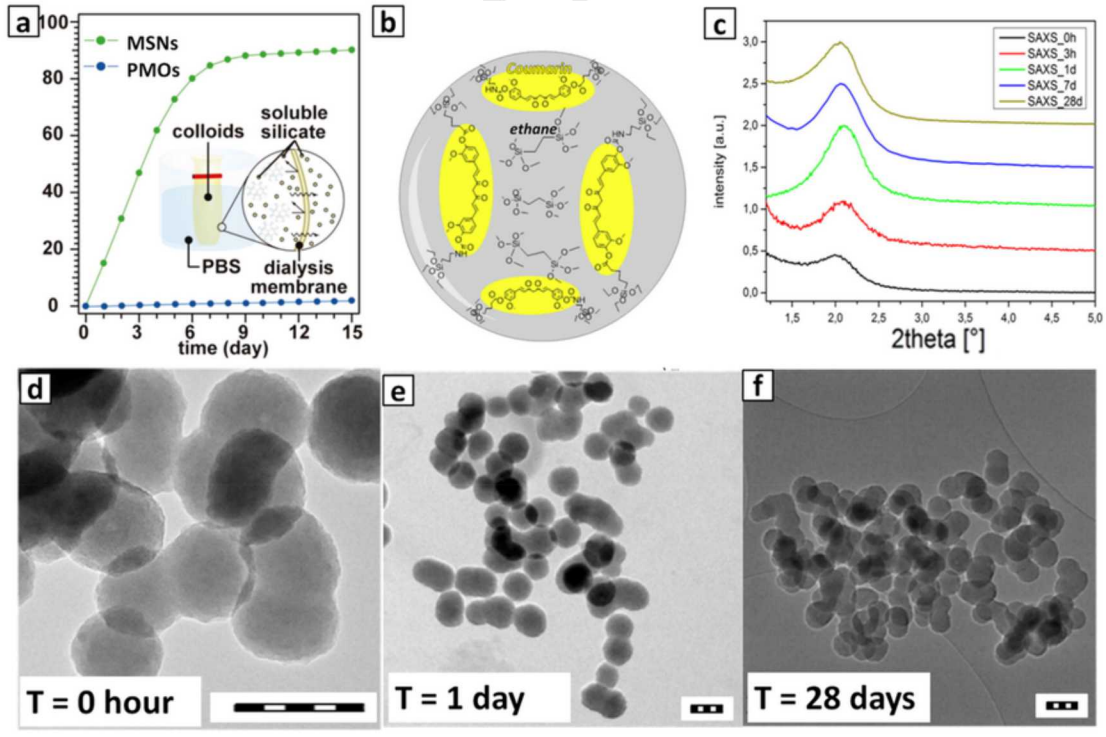

Fig. 8. a) Dissolution behavior of MSN and PMO in a PBS solution for 15 days. The inset illustrates the scheme of this experiment. PMO was aggregated in the solution after 24 h. b) a schematic representation of ethane-coumarin PMO nanoparticles and their degradation-resistant behavior in SBF monitored overtime by c) SAXS and d1-d3) TEM. a) Adapted with permission from [12]. Copyright (2011) American Chemical society. b-d) reproduced with permission [17]. Copyright, 2013, Elsevier.

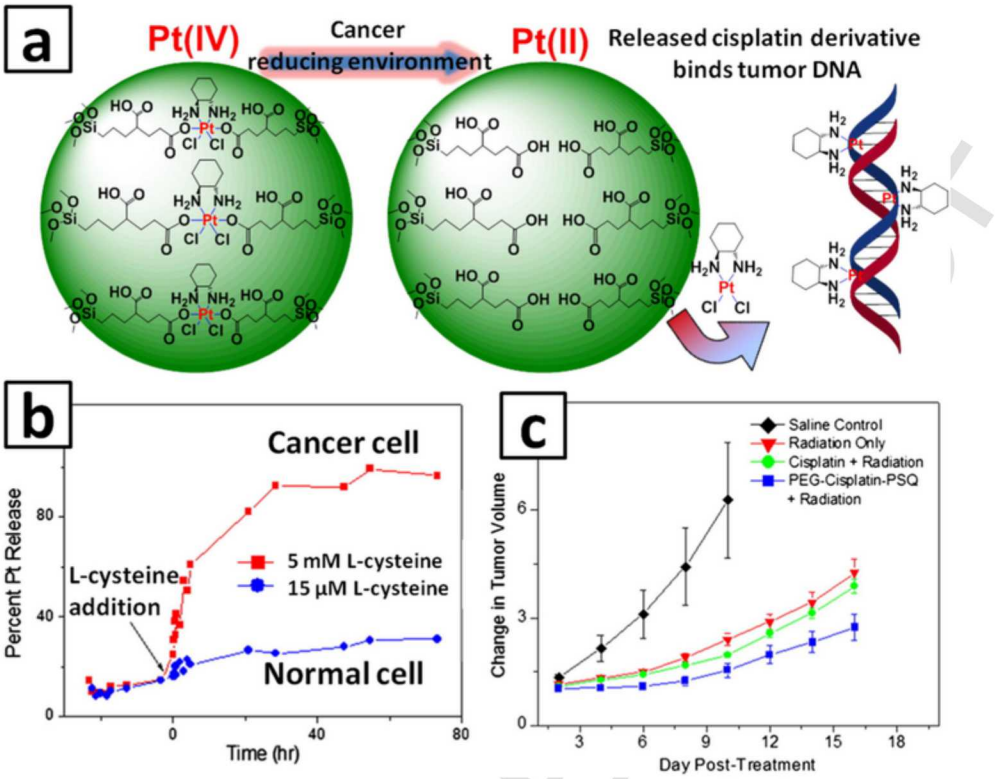

Fig. 9. a) A schematic describing the release mechanism of Pt from BSQ upon exposure to reducing conditions. The released oxaplatin bearing active Pt^{II} will bind to DNA inhibiting tumor growth. b) Release profile of Pt after addition of L-cysteine with amounts mimicking those of normal and cancer cells. c) Evolution in tumor volume over 2 weeks upon exposure to different conditions (control, radiation only, free cisplatin + radiation and Pt-BSQ + radiation). Adapted with permission [18]. Copyright, 2015, Elsevier.

H460 xenografts subjected to chemoradiotherapy. Importantly, the PEGylated system showed superior results compared to other usually administered treatments where the measured tumor volume was 400%, 35% and 25% smaller than the control (saline solution), radiation only, and free cisplatin combined with 10 Gy radiation treatments, respectively (Fig. 9c), thus confirming that these novel BSQ nanoparticles hold a promising role in the development of efficient tumor treatment. It is noteworthy that the same group also reported, based on the same concept, gadolinium-based BSQ nanoparticles for the release of Gd as a contrast agent for MRI [249].

Croissant et al. have shown the synthesis of mixed PMOs with ethenylene (E) and disulfide (DIS) bridges with different weight percentages (*wt* E/DIS = 100/0, 90/10, 75/25, 50/50, 0/100). The shape (600 nm rods to 150 nm spheres) and the aspect ratio (5 to 1) of the nanoparticles were fine-tuned additionally [191]. However, when 100% DIS was used, a non-porous BSQ was obtained instead of PMO material most likely because of the relative complexity of the DIS organic bridge and that ethenylene groups are necessary to confer porosity to the organosilica skeleton. With PMOs obtained with lower E/DIS ratio, an exceptional drug loading (20% *wt* DOX) was achieved due to the hydrophobic character of the PMO pore interiors combined with loading at acidic pH where the silanol protons were exchanged by the positively charged DOX, thus confirming the pH-dependence of DOX loading/release according to an earlier report [216].

Herein, the presence of disulfide-containing bridges endowed the PMOs with an active response to reducing conditions. For this purpose, β-mercaptoethanol was used in extra- and intra-cellular concentrations (6 μM and 2 mM in PBS, respectively) in order to simulate the higher concentration of glutathione present in the cancer environment (1–10 mM) than in normal cells (Fig. 10a). Upon exposure of PMOs to the above mentioned reducing conditions for 48 h, a dissolution behavior was observed in the first hours by TEM (Fig. 10b1–b3) then fragments of silica were detected accompanied by a size decrease in DLS, thus confirming the degradation behavior of disulfide-containing PMOs triggering the release of doxorubicin molecules at lysosomal pH 5.5 (Fig. 10c) into breast cancer MCF-7 cells inducing significant cell death (up to 80% after 72 h incubation at 1 μg/mL) (Fig. 10c1, c2).

In a way to show the versatility of organosilica, Chen, Meng and coworkers have constructed a multi-hybridized hollow organosilica nanoparticle through silica etching chemistry. These latter were then coated in situ by a mixture of two (phenyl and tetrasulfide) (Fig. 11a) and up to five homogeneously distributed organosilanes (ethane-, ethylene-, phenyl-, bisphenyl- and tetrasulfide-bridged bistriethoxysilane) under basic conditions using CTAB as a structuring agent. Dual-hybridized nanoparticles (containing phenylene and tetrasulfide fragments) were then efficiently loaded (~15%*wt*) with doxorubicin due to the π-π stacking and hydrophobic character of the guest molecule. Additionally, owing to the biologically-active [250] tetrasulfide fragments implemented in the shell network, these nanoparticles will present a specific response to reducing environments. The pH-triggered DOX release was monitored at different glutathione concentrations (Fig. 11b) and showed up to a 70% release at [GSH] = 10 mM versus less than 20% in the absence of a reducing agent. The release assisted by particle degradation is also confirmed by TEM where "broken" particles appeared from the first day of incubation and became more pronounced overtime (Fig. 11c-f).

More recently, an enzymatically-cleavable phenylene-oxamide PMO was reported. This system relies on the capability of the trypsin enzyme to break up amino acids [246]. Due to the high extent of phenylene within the framework, an exceptional compothecin (CPT) and doxorubicin loading (up to 80% and 65% *wt* respectively) was achieved. Interestingly, the DOX was not released at lysosomal pH in contrast with what was observed with ethylene-disulfide PMOs suggesting thus a specific interaction between oxamide moieties and drugs.

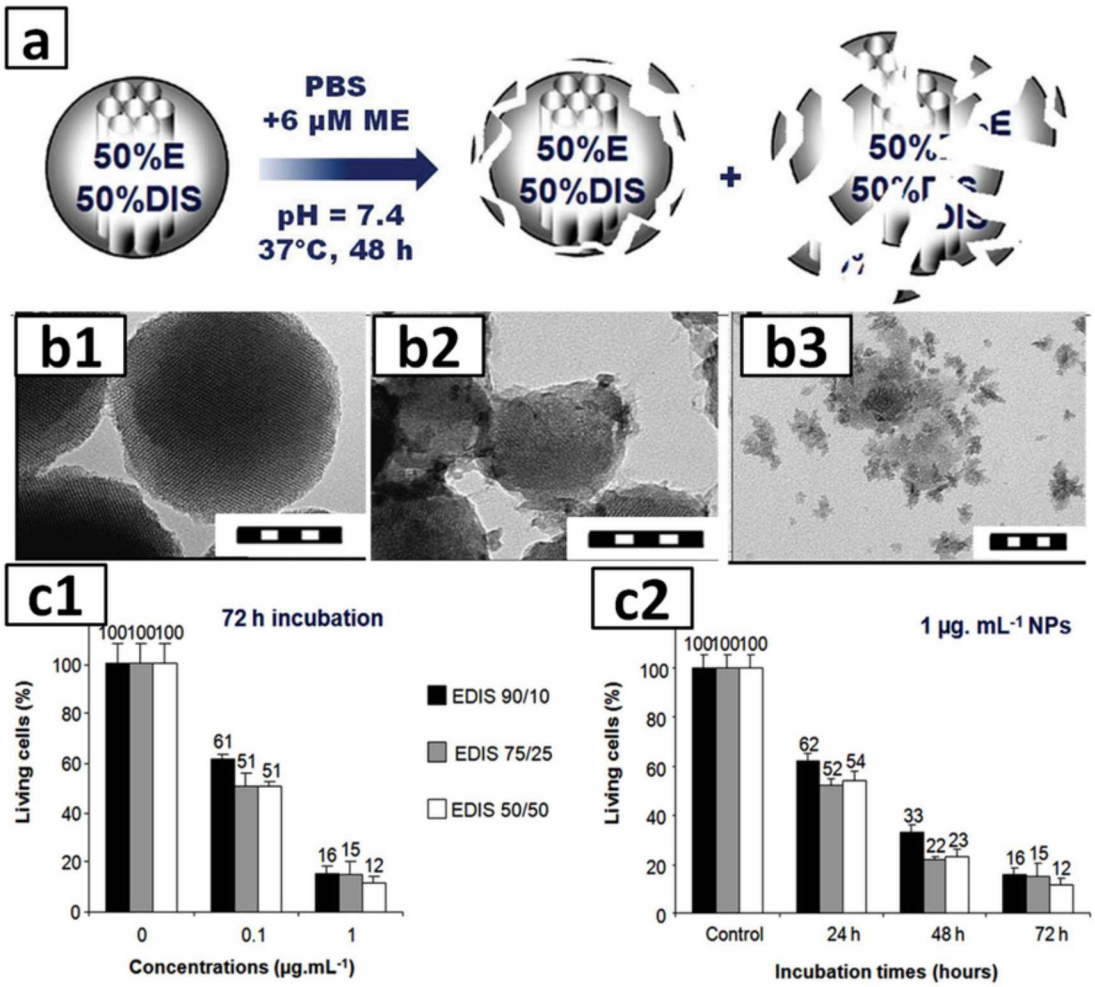

Fig. 10. a) A schematic of the degradation behavior of 50% disulfide PMO under simulated physiological conditions. TEM images of EDIS 50/50 nanospheres before (b1) and after 48 h of degradation under physiological conditions (b2, b3), scale bar = 100 nm. c) In-vitro cytotoxicity studies of EDIS NPs loaded with DOX in acidic conditions for a given incubation time (72 h) and various NPs concentrations (c1), or for a given NPs concentration (1 µg/mL) and various incubation times (c2). Adapted with permission [11]. Copyright 2014, Wiley-VCH.

The release of drugs was only triggered upon exposure of nanoparticles to a trypsin-containing solution for 48 h. This system showed important *in vitro* controlled A549 lung cancer cell killing (65% and 85% with DOX and CPT-laden nanoparticles, respectively).

It is noteworthy that other degradable systems through redox [191] or enzymatic cleavage mechanisms [190] were also synthesized. However, the relative complexity of the introduced organosilanes in the used synthetic conditions was a barrier to make porous structures. The obtained degradable BSQ were though used in nanomedicine for imaging, and photodynamic therapy.

4.3. External stimuli: light-induced release

Although the most abundant work on drug release from silsesquioxanes was carried out based on internal stimuli-triggered release, a few original works were recently reported using external stimuli to induce the cargo release.

4.3.1. Release of hydrogels with antibody-like affinity

In 2012, Shea presented an original approach for light-induced release of "externally" loaded biomolecules [251]. A neutral nitrobenzyl-carbamate bisilylated organosilane was used to make 250 nm dense BSQ nanoparticles. Upon light excitation ($\lambda = 254$ nm), the carbamate link is cleaved, inducing the removal of nitrobenzyl cycle and leaving positively charged amine moieties covering the complete organosilica framework (Fig. 12a). The original zeta potential of the nanoparticles ($\zeta = -40$ mV) starts increasing directly after excitation and Increased to $\zeta = +30$ mV after 20 min irradiation.

This phenomenon was first demonstrated by a light-induced coverage of the BSQ surface with 70 nm negatively charged silica nanoparticles *via* an electrostatically mediated process (Fig. 12a-c). In order to prove the release potential of the system, a positively charged (PA + 74) polyacrylamide copolymer hydrogel nanocomposites ($\zeta = +37$ mV, size = 74 nm) presenting antibody-like affinity to peptides [252,253], were adsorbed on the surface through electrostatic attraction. The Light-controlled charge reversal of BSQ induced charge repulsion of the antibodies resulting in their quick light-triggered release (Fig. 12d).

4.3.2. DNA release

Following this light-induced charge-reversal concept, Khashab et al. synthesized hollow BSQ using a photo-responsive bisilylated nitrobenzyl-based organosilane [254] (Fig. 13a). In contrast to the previous study, this organic fragment is positively charged in water and has the ability to become neutrally charged upon light excitation (Fig. 13b). This characteristic was smartly used to load highly negative plasmid DNA *via* electrostatic interaction with the highly positive BSQ ($\zeta = +46$ mV) (Fig. 13b-e). Upon one-photon light excitation, the ni-

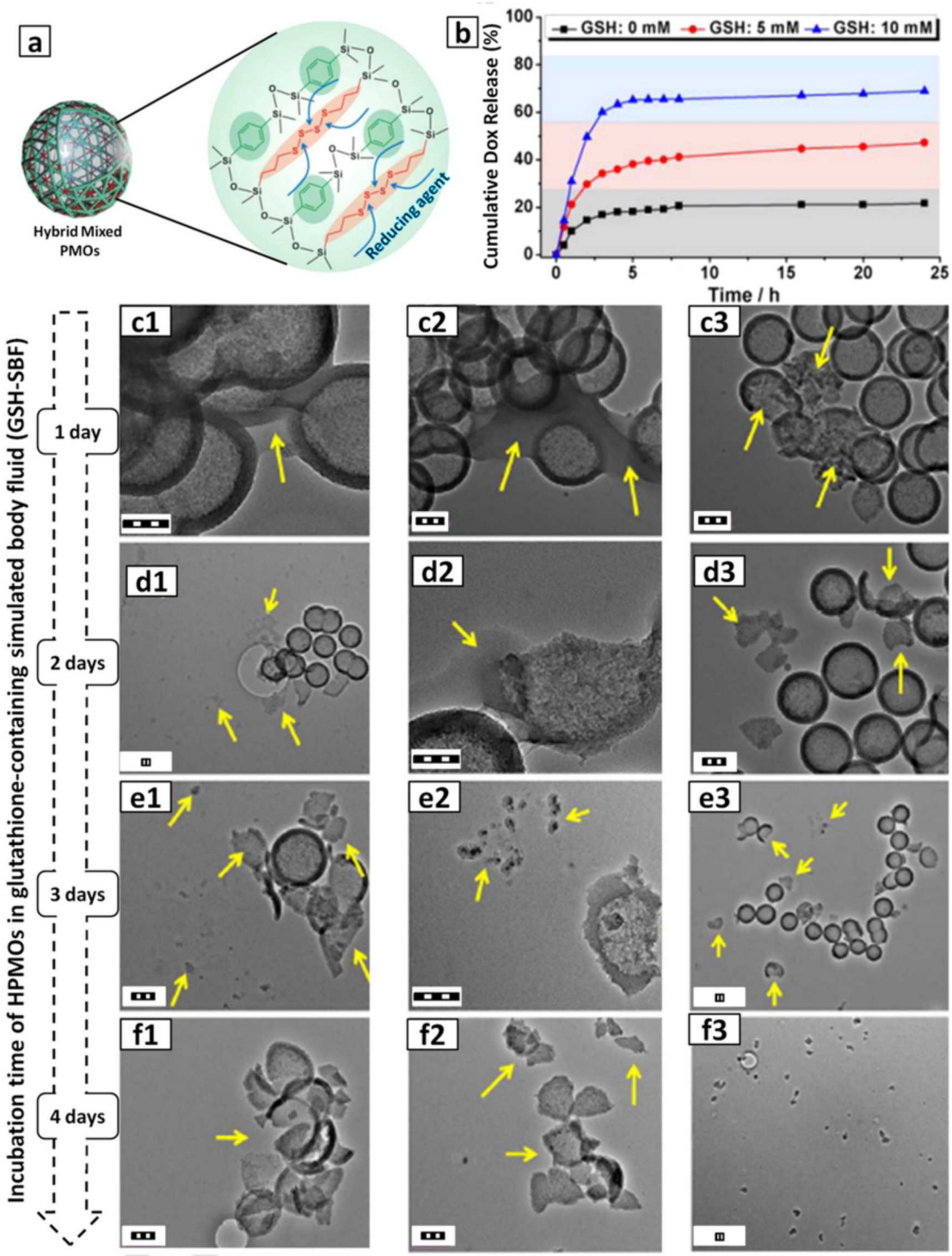

Fig. 11. a) Schematic illustration of the framework composition of dual-hybridized HPMOs (thioether, phenylene). b) Cumulative Dox-release percentages at GSH concentrations of 0, 5, and 10 mM in PBS solutions. (c-f) Biodegradation behavior of HMONs in simulated body fluid (SBF) at GSH concentration of 10 mM for (c) 1d, (d) 2d, (e) 3d and (f) 4d. TEM images of HMONs after treatment in GSH-containing SBF for (c1-c3) 1d, (d1-d3) 2d, (e1-e3) 3d and (f1-f3) 4d, scale bar = 100 nm. Adapted with permission from [19]. Copyright (2014) American Chemical Society.

trobenzyl fragments turn neutral, and the charge of the BSQ is mainly represented by the negatively charged deprotonated surface silanol groups ($\zeta = -39$ mV) (Fig. 13b). This charge reversal phenomenon induced the release of DNA by strong charge repulsion (Fig. 13e) and was then applied *in vitro* on MCF-7 cells. The delivery (and transcription) of DNA into cell nuclei (to translate mRNA) was successfully assessed by the production of GFP (used as a reporter protein). (Fig. 13f,g)

The uncontrolled release of cargo has always been problematic for applications of nanosystems in biology [255]. For example, as for silica, Zink [19,21,256,257], Lin [229,234,236] and Bein [25,258,259] were very active in innovating so-called nanomachines [25,234,260-266] in order to prevent payload leakage and enable triggered release.

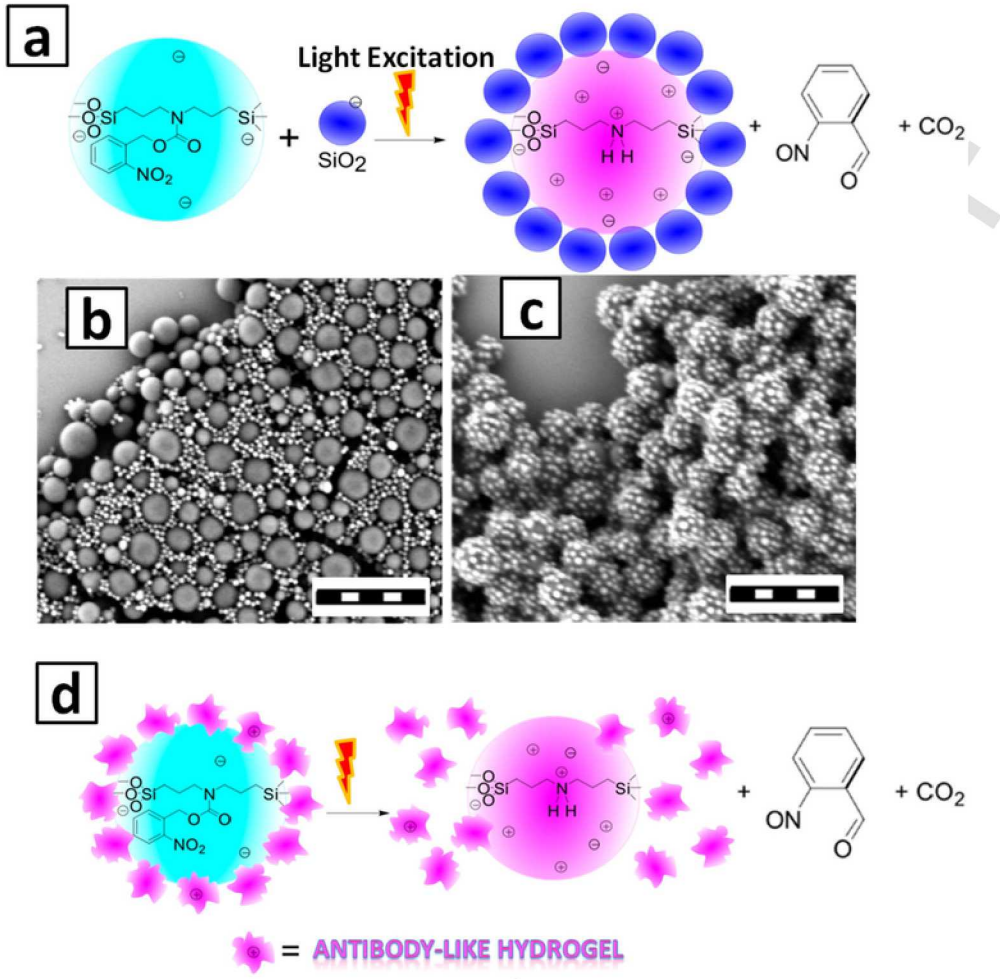

Fig. 12. a) Schematic of light-triggered charge reversal and chemistry of nitrobenzyl-carbamate BSQ and "NP Shell" Assembly. SEM image of centrifuged, resuspended, and dried mixture of (BSQ 260 nm) and (SiO_2 70 nm) (b) before and (c) after UV irradiation. Scale bar: 1 μm. d) Light-Triggered Release of antibody-like hydrogel. Adapted with permission from [20]. Copyright (2012) American Chemical Society.

As for the silsesquioxanes, various physical interactions with cargos mediated by the organic fragments resulted in better retention. Accordingly, silsesquioxanes can be utilized without any further chemical modification/passivation in order to controllably deliver the payload. This suggests a superiority of silsesquioxane nanoparticles over their silica analogs.

4.4. Comparison with MSNs

Native MSNs, *per se*, cannot be exploited for triggered release at physiological pH requiring functionalization by stimuli-responsive moieties, which could be time-consuming or induce aggregation. Silsesquioxanes, are intrinsically and fully built by organic bridges between siloxanes and they can carry several organic fragments at once. Therefore, they are more appealing for intended triggered release applications. For example, a spontaneous cargo release (via electrostatic repulsion) from silsesquioxanes can take place through a charge reversal phenomenon when the pH turns from neutral to mild acidic under endosomal conditions.

Although it is theoretically possible to post-functionalize MSNs by any organic functions, the superior amount of active moieties within a silsesquioxane remains more advantageous in most of the cases.

5. Hierarchically-built systems for synergistic drug release

The production of nanosystems with increasing complexity is constantly being pursued in order to overcome complexity of biological systems, but especially to develop a system entirely capable of imaging and eradication of malignant tumors. In this section we will see how different complex systems were developed not only to load and release drugs with opposite characteristics (e.g. hydrophobic and hydrophilic), but also by combining this release with imaging or other techniques that synergistically diagnose, image and kill cancer cells.

5.1. Dual release of therapeutics

5.1.1. Hydrophilic and hydrophobic

Zhao, Zhang et al. presented an original approach for hierarchically-built Janus nanoparticles [267] starting from "seeds" of gadolinium-based ($NaGdF_4$:Yb,Tm@$NaGdF_4$) upconversion quantum dots (UCQD) separated from a mesoporous silica shell by a dense non-porous silica layer in order to chemically-protect UCQD (Fig. 14a). Over the mesoporous shell of the obtained spherical core (island), ethylene bridged organosilane undergoes a sol-gel process to yield a cubic PMO attached to the spherical island *via* an unprecedented anisotropic island nucleation and growth process (Fig. 14a,b). The co-existence of silica and organosilica matrices herein, allowed the system to house si-

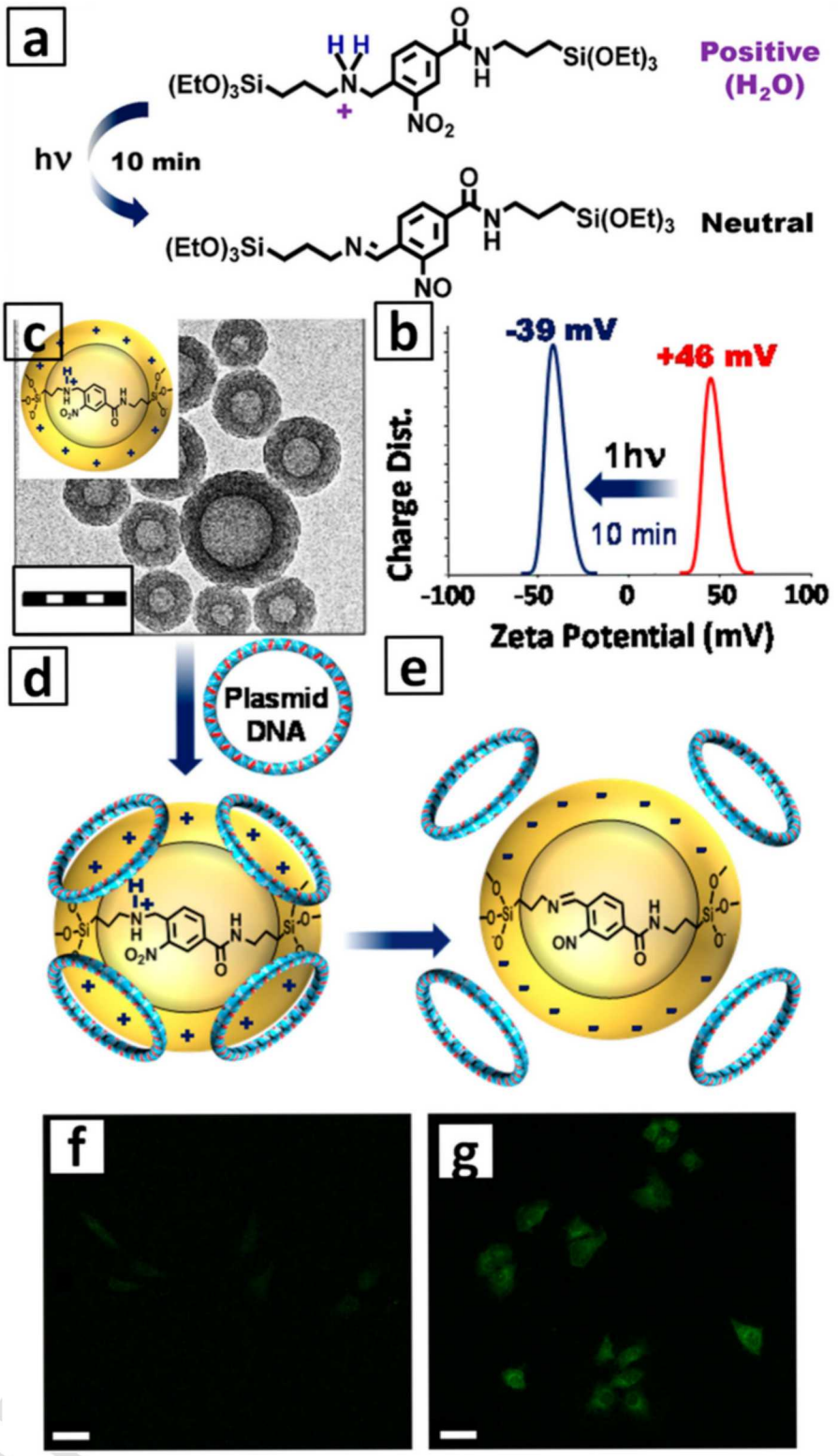

Fig. 13. a) Schematic representing the photoreaction of the nitrobenzyl bisilylated precursor b) ζ potential measurements on BSQ NPs before and after irradiation, depicting the NP surface charge reversal. c-e) Schematic representation and TEM image of positively charged BS NPs, scale bar = 100 nm (c) that electrostatically bind DNA strands (d) for light-triggered delivery (e). The negative charge of NPs results from neutralization of the charge of organic bridges. (f-g) Confocal laser scanning microscopy images of HeLa cells incubated with BS NPs binding DNA strands after 6 h of incubation (g). DNA is tracked via green fluorescent protein (GFP) fluorescence after translation in the nuclei, thus proving the DNA delivery from BSQ. Before irradiation (f), a low GFP signal was monitored, indicating that some DNA was autonomously delivered to cells. Scale bars = 40 μm. Adapted with permission from [21]. Copyright (2015) American Chemical Society.

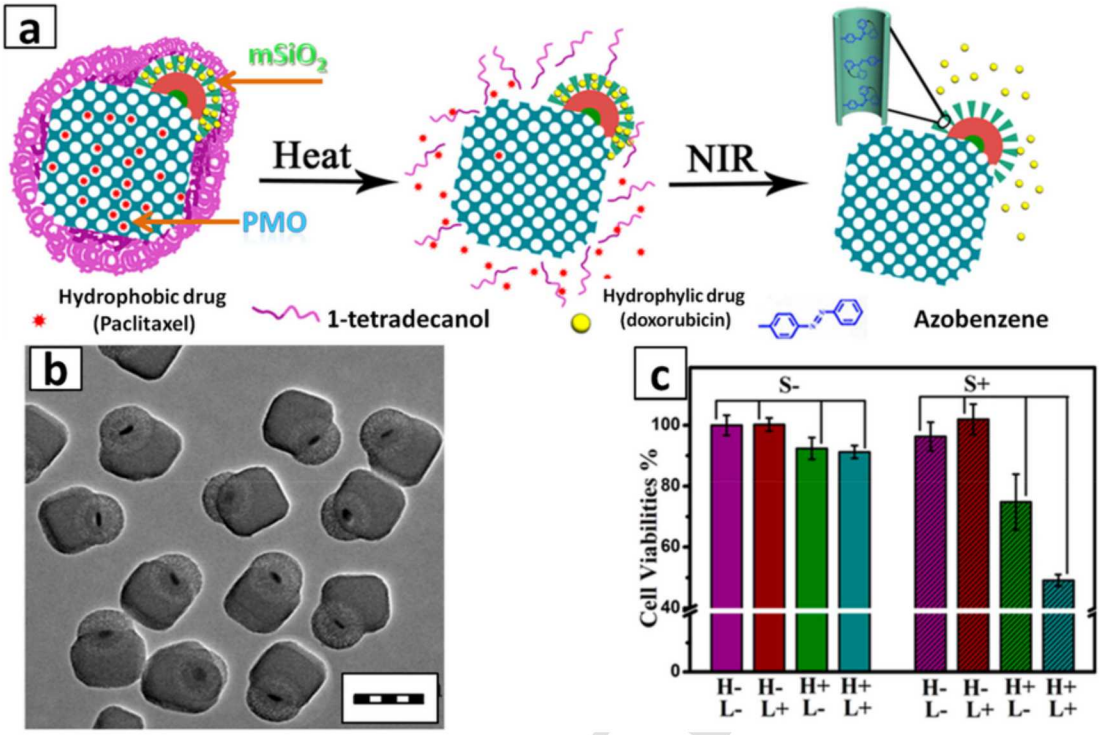

Fig. 14. A) Schematic illustration of dual-controlled drug release systems using the dual-compartment mesoporous Janus nanocomposites UCQD@SiO_2@mSiO_2@PMO b) TEM of the Janus nanocomposite, scale bar = 200 nm. c) Cell viabilities of paclitaxel and DOX co-loaded UCQD@SiO_2@mSiO_2-Azo&PMO–tetradecanol Janus nanocomposites under (+) or without (−) heat (H) and NIR light (L) treatment (S = sample). Adapted with permission from [22]. Copyright (2014) American Chemical Society.

multaneously hydrophilic (DOX) and hydrophobic (paclitaxel) drugs. In addition, this novel system possesses quantum dot nuclei, allowing the absorption of NIR light and the emission of visible wavelength. This feature was intelligently harnessed by inserting azobenzene moieties in the pores of the mesoporous silica shell. Azobenzene is a well known as 'gatekeeper' for 2–3 nm sized pores and, due to reversible photoisomerization from *cis* to *trans* confirmations, serves as an impeller to promote cargo release upon UV/vis light exposure [18,204,266,268–271]. Moreover, in order to seal the whole Janus nanosystem, heat-sensitive tetradecanol was used as a coating (Fig. 14a). *In vitro* assays on HeLa cells were then performed with exposing the dual-loaded particles to heat and/or light (Fig. 14c). The cell viability assays showed 1) excellent biocompatibility of the system 2) no effect when only light was on, simply because the heat-sensitive tetradecanol was still sealing the pores and no drug was able to reach the cells. However, at least 25% cell death occurred upon heat exposure only, due to the release of the paclitaxel from PMO pores. Importantly, upon light and heat excitation, both drugs were released and more than 50% cell death was observed. These results demonstrate the ability to create complex functionality wherein drugs with opposite hydrophilic/phobic characters can be loaded and independently released according to a logic system depending on specific stimuli.

5.1.2. Bimodal

Shortly later, and based on the same concept, this group reported crescent-like eccentric "hollow" Janus constructs by post-etching a dense silica core [272]. This hollowness, also called a single-hole is open to the surface and can then bear large molecules. BSA proteins were housed therein, sealed by heat-sensitive coating, and DOX found shelter in the mesoporous shell. Again, the controlled dual release was successfully demonstrated upon heat and NIR stimuli.

5.2. Photodynamic therapy (PDT) and imaging with synergistic drug release

Durand and co-workers pioneered the development of PMO mixed systems with metal cores and two-photon photosensitizers and porphyrins embedded in the silsesquioxane framework, for 2 photon imaging, photodynamic therapy and synergistic drug release.

In situ gold/(ethylene or benzene-based) PMO nanoparticles embedded with a 2-photon (2hν) sensitizer were produced [273] by co-condensation. The 2hνmoiety provides the photodynamic therapy functionality, which is highly enhanced by the presence of Au cores. Drug-free or DOX-loaded nanoparticles were incubated with MCF-7 cells and afterward exposed or not to 2hν-irradiation (Fig. 15a). Cell assays (Fig. 15b,c) show that even without any drug loaded, a cell killing was induced (up to 40% for AE2 only due to PDT). For drug-loaded nanoparticles, an autonomous drug release induced 40–45% cell death without any PDT effect (laser off) and this percentage increased up to 76% after the laser was turned on, thus beautifully highlighting the synergistic effects of drug release and PDT on these Au-2hν-PMOs nanocomposites.

In another example, octasilylated Zn-porphyrin (bearing 8 triethoxysilanes) prepared by CuAAC click chemistry [40,274-284] was cocondensed with bisilylated ethylene group to produce 460 nm nanoparticles [285]. Due to its large size and π-π stacking, the porphyrin aggregated in the framework and allowed two-photon imaging with low laser power for MCF-7 cancer cells. This latter feature was highlighted in parallel to an autonomous release of drug in the cancer environment. Later on, the same group prepared nanodiamond cores surrounded by ethane or ethylene based-PMO shells [183] (separated by a thin silica layer) and they demonstrated that the photodynamic therapy effect increased from 40% to up to 87% cell killing when synergistically combined with pH-induced drug release. Interestingly, this

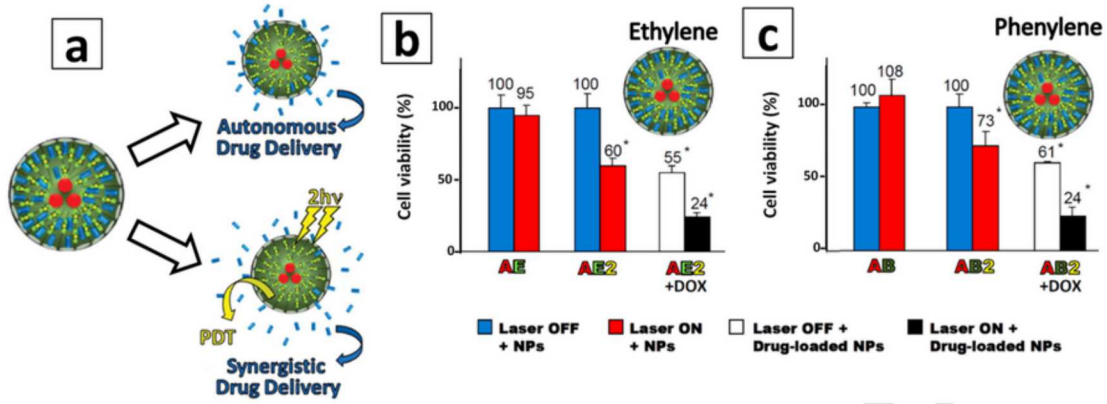

Fig. 15. a) Autonomous drug delivery and 2-photon excitation-PDT combined with synergistic drug delivery. Demonstration of the synergistic effect of two-photon photodynamic therapy (PDT) and drug delivery, via DOX-free Au@PMO, Au@PMO-2hν, and DOX-loaded Au@PMO-2hν for b) ethylene- and c) benzene-bridged PMO. (A: gold cores, E: Ethylene, B: Benzene, 2: 2-photon sensitizer, DOX: doxorubicin) Adapted with permission from [2]. Copyright (2014) American Chemical Society.

system indicated that reactive oxygen species (ROS) were produced and detected following nanodiamond 2hν excitation.

5.3. High intensity focused ultrasound-HIFU with synergistic drug release

HIFU (Fig. 16a) is an FDA-approved technique used to burn prostate cancer [286]. However, this technique may cause invasive ablation or damage to surrounding healthy tissues. Here again, the diverse functionalities of PMOs can help address this problem. HIFU-assisted release was demonstrated by Chen et al. [287] using previously described DOX-loaded tetrasulfide-phenylene HPMOs [168] (Fig. 11a). In fact, the π-π interaction between DOX and aromatic phenylene is sensitive to focused ultrasound and will be significantly weakened upon HIFU application. In addition, it has been demonstrated on MSN and polymer micelles that cleavage of disulfide bonds can occur under similar conditions [288-290]. These features were therefore harnessed to actuate the HIFU-triggered controlled drug release from these HPMOs nanocapsules (Fig. 16b).

In addition, HPMOs were successfully used in contrast-enhanced ultrasonography and HIFU-assisted release of paclitaxel-laden HPMOs exhibited better tumor inhibition rates than free drug and loaded HPMOs without ultrasound [291].

Importantly, HIFU assisted drug release has been also applied *in vivo* where DOX loaded HPMOs were intratumorally injected in ICR mice (n = 20) with rat sarcoma S-180 xenografts [292]. The exposure to nanoparticles took place 2 weeks after the xenograft (when tumor volume reached around 15 mm^3). Mice with and without HPMO injections were also exposed to HIFU (200 W, 10 s). The volume of the tumor was monitored every 2 days for 15 days (Fig. 16c). A synergistic effect of HIFU hyperthermia and drug release to inhibit tumor growth was demonstrated: while tumors exposed solely to HIFU or DOX-HPMOs resulted respectively in 34 or 59 wt% tumor growth inhibition, the combined synergistic effect of HIFU and HPMOs exhibited up to 73 wt% inhibition compared to non-treated tumors (Fig. 16c,d).

In summary, HIFU, PDT and biocompatible 2hν-imaging were proven to be very effective when combined with the capacity of silsesquioxanes to deliver drugs. In the future, it will be of high impor-

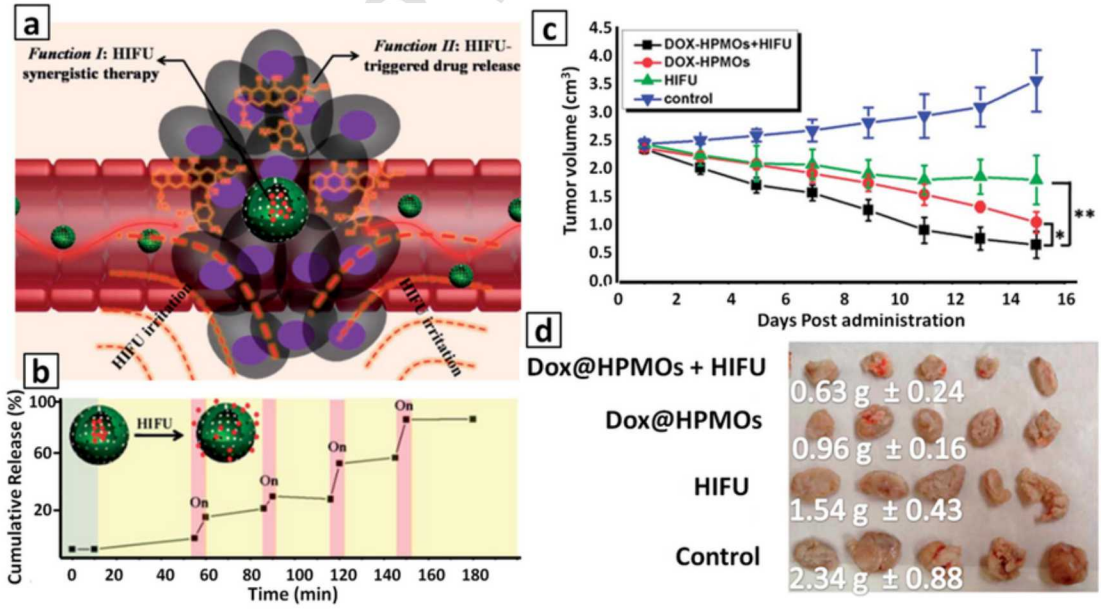

Fig. 16. a) Schematic illustration of HPMO-based HIFU synergistic therapy combined with HIFU-triggered drug release. b) drug-release from DOX-loaded HPMOs under HIFU irritation (200 W) c) changes of tumor volume as a function of time after different treatments (control, HIFU irradiation, DOX–HPMOs and DOX HPMOs combined with HIFU irradiation), ($^{*}P < .05$, $^{**}P < .01$) in ICR mice implanted with rat sarcoma S-180 (n = 5), d) digital pictures of tumors at the end of therapy under different treatments with the corresponding tumor weight. Adapted from Adapted with permission [23]. Copyright 2014, Royal Society of Chemistry.

tance to take advantage of such systems in order to deliver more complex payloads like biomolecules capable of gene silencing or editing.

6. Conclusion and insights

Functional organic and inorganic fragments synergistically exist in each unit of the silsesquioxane framework building blocks plethora, enabling the development of NPs with diverse and complex characteristics. The homogeneous distribution of organic moieties and their extensive physicochemical input endows the material with new properties. Clever means of therapeutic release were demonstrated by pendant and bridged silsesquioxanes through different internal (cancer μ-environment mimics) and external (light) stimuli. Electrostatic repulsion/destabilization by pH drop or light-induced charge reversal as well as reductive framework cleavage were brilliantly used to trigger drug release. Other functions used in biomedicine (photodynamic therapy, imaging, high intensity focused ultrasound) were combined to achieve synergistic drug release. Silsesquioxane presents easy fine-tuning of the framework/pore surface properties (hydrophobic, electrostatic, H-bond, π-π interactions), enabling a superior loading efficiency and correspondingly a lower required administered dose.

Silsesquioxane nanoparticles are fundamentally different than MSN on the structural level as they are entirely built by organic bridges separating the siloxanes. The uniform distribution of organic fragments endows silsesquioxanes with a superior activity compared to MSNs. The possibility to create mixed silsesquioxanes (containing several organosilanes moieties) also paves the way into synergistic applications and possibly new morphologies. Although the production of monosized and porous silsesquioxane nanoparticles with large pore size and pore volume remains highly challenging compared to straightforward and widely-studied MSNs, different PSQ, BSQ and PMOs have demonstrated incredible capabilities in biology. Silsesquioxanes exhibit comparable biocompatibility to MSNs and even better hemocompatibility due to their reduced concentrations of surface silanols. However due to their lower silanol content and the reduced acidity of silanols, silsesquioxanes have a higher isoelectric point and reduced charge compared to MSNs resulting in lower stability in nearly neutral conditions and different surface charge when exposed to the same conditions (i.e. neutral pH). This latter feature was exploited for payload release through spontaneous charge reversal, without any further functionalization, which is unique for silsesquioxanes.

In spite of the great chemical versatility of silsesquioxane nanocarriers, we found a lack in the literature of loading uncommon drug molecules. Also in order to shed more light on mesoporous silsesquioxane nanoparticles, reproducible synthesis with large pores capable of accommodating larger and more charged biomolecules is an urgent need and will be a brilliant advance in the field. Research on BSQ and PMOs should be pushed towards "combo combat" [293] to achieve co-delivery of multiple components like drug/siRNA to suppress drug efflux and reduce multiple drug resistance mechanisms, but also, like inhibitors/cytokines to inhibit/delay tumor growth thus increasing the efficiency of natural killer cells [294].

Overall, although silsesquioxane nanosystems exhibit several advantages over the MSNs, we estimate that it is too early to talk about a complete superiority of the pure organosilica as more research is still needed to resolve problems and upscale their syntheses as well as understand the potential relationship between individual silsesquioxane frameworks with bio-relevant systems.

However, we believe that in the near future potent mesoporous silsesquioxane nanoparticles will bring novel solutions to existing problems. Maybe the dawn of silsesquioxanes arose due to scientific curiosity but they now promise to solve complex problems in delivery of different molecules of interest.

Acknowledgment

This work was supported by the Sandia National Laboratories' Laboratory Directed Research and Development (LDRD) program and the Lymphoma and Leukemia Society (LLS) (A.N. and C.J.B.). Sandia National Laboratories is a multi-mission laboratory managed and operated by National Technology and Engineering Solutions of Sandia, LLC, a wholly owned subsidiary of Honeywell International, Inc., for the U.S. Department of Energy's National Nuclear Security Administration under contract DE-NA0003525.

References

[1] J.F. Batlle, E.E. Arranz, J. de C. Carpeño, E.C. Sáez, P.Z. Auñón, A.R. Sánchez, et al., Oral chemotherapy: potential benefits and limitations, Clin. Transl. Oncol. 6 (2004) 335–340, https://doi.org/10.1007/BF02710062.
[2] S.P. Egusquiaguirre, M. Igartua, R.M. Hernández, J.L. Pedraz, Nanoparticle delivery systems for cancer therapy: advances in clinical and preclinical research, Clin. Transl. Oncol. 14 (2012) 83–93, https://doi.org/10.1007/s12094-012-0766-6.
[3] T. Iwamoto, Clinical application of drug delivery systems in cancer chemotherapy: review of the efficacy and side effects of approved drugs, Biol. Pharm. Bull. 36 (2013) 715–718, https://doi.org/10.1248/bpb.b12-01102.
[4] T.M. Allen, Drug delivery systems: entering the mainstream, Science 303 (2004) 1818–1822, https://doi.org/10.1126/science.1095833.
[5] B.S. Pattni, V.V. Chupin, V.P. Torchilin, New developments in liposomal drug delivery, Chem. Rev. 115 (2015) 10938–10966, https://doi.org/10.1021/acs.chemrev.5b00046.
[6] Q. Yang, R. Qi, J. Cai, X. Kang, S. Sun, H. Xiao, et al., Biodegradable polymer-platinum drug conjugates to overcome platinum drug resistance, RSC Adv. 5 (2015) 83343–83349, https://doi.org/10.1039/c5ra11297d.
[7] Y. Zhang, P. Lundberg, M. Diether, C. Porsch, C. Janson, N.A. Lynd, et al., Histamine-functionalized copolymer micelles as a drug delivery system in 2D and 3D models of breast cancer, J. Mater. Chem. B 3 (2015) 2472–2486, https://doi.org/10.1039/C4TB02051K.
[8] L. Yang, X. Hu, W. Wang, S. Liu, T. Sun, Y. Huang, et al., Y-shaped block copolymer (methoxy-poly(ethylene glycol))?n2?n-b-poly(?n l?n-glutamic acid): preparation, self-assembly, and use as drug carriers, RSC Adv. 4 (2014) 41588–41596, https://doi.org/10.1039/C4RA07890J.
[9] J. Xu, Q. Zhao, Y. Jin, L. Qiu, High loading of hydrophilic/hydrophobic doxorubicin into polyphosphazene polymersome for breast cancer therapy, Nanomed. Nanotechnol. Biol. Med. 10 (2014) 349–358, https://doi.org/10.1016/j.nano.2013.08.004.
[10] R.E. Serda, A. MacK, M. Pulikkathara, A.M. Zaske, C. Chiappini, J.R. Fakhoury, et al., Cellular association and assembly of a multistage delivery system, Small 6 (2010) 1329–1340, https://doi.org/10.1002/smll.201000126.
[11] S. Ferrati, A. Mack, C. Chiappini, X. Liu, A.J. Bean, M. Ferrari, et al., Intracellular trafficking of silicon particles and logic-embedded vectors, Nanoscale 2 (2010) 1512, https://doi.org/10.1039/c0nr00227e.
[12] R.E. Serda, A. MacK, A.L. Van De Ven, S. Ferrati, K. Dunner, B. Godin, et al., Logic-embedded vectors for intracellular partitioning, endosomal escape, and exocytosis of nanoparticles, Small 6 (2010) 2691–2700, https://doi.org/10.1002/smll.201000727.
[13] D.J. Savage, X. Liu, S.A. Curley, M. Ferrari, R.E. Serda, Porous silicon advances in drug delivery and immunotherapy, Curr. Opin. Pharmacol. 13 (2013) 834–841, https://doi.org/10.1016/j.coph.2013.06.006.
[14] K.I. McConnell, J. Rhudy, K. Yokoi, J. Gu, A. Mack, J. Suh, et al., Enhanced gene delivery in porcine vasculature tissue following incorporation of adeno-associated virus nanoparticles into porous silicon microparticles, J. Control. Release 194 (2014) 113–121, https://doi.org/10.1016/j.jconrel.2014.08.020.
[15] R. Elia, D.R. Newhide, P.D. Pedevillano, G.R. Reiss, M.A. Firpo, E.W. Hsu, et al., Silk-hyaluronan-based composite hydrogels: a novel, securable vehicle for drug delivery, J. Biomater. Appl. 27 (2011) 749–762, https://doi.org/10.1177/0885328211424516.
[16] K.S. Butler, P.N. Durfee, C. Theron, C.E. Ashley, E.C. Carnes, J. Brinker, Protocells: modular mesoporous silica nanoparticle-supported lipid bilayers for drug delivery, Small 12 (2016) 1–13, https://doi.org/10.1002/smll.201200042.
[17] P.N. Durfee, Y.S. Lin, D.R. Dunphy, A.J. Muñiz, K.S. Butler, K.R. Humphrey, et al., Mesoporous silica nanoparticle-supported lipid bilayers (protocells) for active targeting and delivery to individual leukemia cells, ACS Nano 10 (2016) 8325–8345, https://doi.org/10.1021/acsnano.6b02819.
[18] S. Angelos, M. Liong, E. Choi, J.I. Zink, Mesoporous silicate materials as substrates for molecular machines and drug delivery, Chem. Eng. J. 137 (2008) 4–13, https://doi.org/10.1016/j.cej.2007.07.074.
[19] D. Tarn, C.E. Ashley, M. Xue, E.C. Carnes, J.I. Zink, C.J. Brinker, Mesoporous silica nanoparticle nanocarriers: biofunctionality and biocompatibility, Acc. Chem. Res. 46 (2013) 792–801, https://doi.org/10.1021/ar3000986.
[20] Z. Li, J.C. Barnes, A. Bosoy, J.F. Stoddart, J.I. Zink, Mesoporous silica nanoparticles in biomedical applications, Chem. Soc. Rev. 41 (2012) 2590, https://doi.org/10.1039/c1cs15246g.
[21] M.W. Ambrogio, C.R. Thomas, Y.L. Zhao, J.I. Zink, J.F. Stoddart, Mechanized silica nanoparticles: a new frontier in theranostic nanomedicine, Acc. Chem. Res. 44 (2011) 903–913, https://doi.org/10.1021/ar200018x.

[22] J. Croissant, J.I. Zink, Nanovalve-controlled cargo release activated by plasmonic heating, J. Am. Chem. Soc. 134 (2012) 7628–7631, https://doi.org/10.1021/ja301880x.
[23] C. Barbé, J. Bartlett, L. Kong, K. Finnie, H.Q. Lin, M. Larkin, et al., Silica particles: a novel drug-delivery system, Adv. Mater. 16 (2004) 1959–1966, https://doi.org/10.1002/adma.200400771.
[24] A. Noureddine, L. Lichon, M. Maynadier, M. Garcia, M. Gary-Bobo, J.I. Zink, et al., Controlled multiple functionalization of mesoporous silica nanoparticles: homogeneous implementation of pairs of functionalities communicating through energy or proton transfers, Nanoscale 7 (2015) 11444–11452, https://doi.org/10.1039/C5NR02620B.
[25] C. Argyo, V. Weiss, C. Bräuchle, T. Bein, Multifunctional mesoporous silica nanoparticles as a universal platform for drug delivery multifunctional mesoporous silica nanoparticles as a universal platform for drug delivery, Chem. Mater. 26 (2013) 435–451, https://doi.org/10.1021/cm402592t.
[26] K. Möller, J. Kobler, T. Bein, Colloidal suspensions of nanometer-sized mesoporous silica, Adv. Funct. Mater. 17 (2007) 605–612, https://doi.org/10.1002/adfm.200600578.
[27] T. Yu, A. Malugin, H. Ghandehari, Impact of silica nanoparticle design on cellular toxicity and hemolytic activity, ACS Nano 5 (2011) 5717–5728, https://doi.org/10.1021/nn2013904.
[28] H. Yamada, C. Urata, Y. Aoyama, S. Osada, Y. Yamauchi, K. Kuroda, Preparation of colloidal mesoporous silica nanoparticles with different diameters and their unique degradation behavior in static aqueous systems, Chem. Mater. 24 (2012) 1462–1471, https://doi.org/10.1021/cm3001688.
[29] T. Yu, K. Greish, L.D. McGill, A. Ray, H. Ghandehari, Influence of geometry, porosity, and surface characteristics of silica nanoparticles on acute toxicity: their vasculature effect and tolerance threshold, ACS Nano 6 (2012) 2289–2301, https://doi.org/10.1021/nn2043803.
[30] Y.S. Lin, C.L. Haynes, Impacts of mesoporous silica nanoparticle size, pore ordering, and pore integrity on hemolytic activity, J. Am. Chem. Soc. 132 (2010) 4834–4842, https://doi.org/10.1021/ja910846q.
[31] X. Huang, L. Li, T. Liu, N. Hao, H. Liu, D. Chen, et al., The shape effect of mesoporous silica nanoparticles on biodistribution in vivo, ACS Nano 5 (2011) 5390–5399, https://doi.org/10.1021/nn200365a.
[32] J. Croissant, A. Chaix, O. Mongin, M. Wang, S. Clément, L. Raehm, et al., Two-photon-triggered drug delivery via fluorescent nanovalves, Small 10 (2014) 1752–1755, https://doi.org/10.1002/smll.201400042.
[33] M.R. Villegas, A. Baeza, M. Vallet-Regí, Hybrid collagenase nanocapsules for enhanced nanocarrier penetration in tumoral tissues, ACS Appl. Mater. Interfaces 7 (2015) 24075–24081, https://doi.org/10.1021/acsami.5b07116.
[34] A. Taguchi, F. Schüth, Ordered mesoporous materials in catalysis, Microporous Mesoporous Mater. 77 (2005) 1–45, https://doi.org/10.1016/j.micromeso.2004.06.030.
[35] P. Yang, S. Gai, J. Lin, Functionalized mesoporous silica materials for controlled drug delivery, Chem. Soc. Rev. 41 (2012) 3679, https://doi.org/10.1039/c2cs15308d.
[36] S. Giret, M. Wong, Chi Man, C. Carcel, Mesoporous-silica-functionalized nanoparticles for drug delivery, Chem. Eur. J. 21 (2015) 13850–13865, https://doi.org/10.1002/chem.201500578.
[37] M. Vallet-Regí, Nanostructured mesoporous silica matrices in nanomedicine, J. Intern. Med. 267 (2010) 22–43, https://doi.org/10.1111/j.1365-2796.2009.02190.x.
[38] K. Suzuki, K. Ikari, H. Imai, Synthesis of silica nanoparticles having a well-ordered mesostructure using a double surfactant system, J. Am. Chem. Soc. 126 (2004) 462–463, https://doi.org/10.1021/ja038250d.
[39] C. Urata, Y. Aoyama, A. Tonegawa, Y. Yamauchi, K. Kuroda, Dialysis process for the removal of surfactants to form colloidal mesoporous silica nanoparticles, Chem. Commun. (2009) 5094–5096, https://doi.org/10.1039/b908625k.
[40] A.T. Dickschat, F. Behrends, M. Bühner, J. Ren, M. Weiß, H. Eckert, et al., Preparation of bifunctional mesoporous silica nanoparticles by orthogonal click reactions and their application in cooperative catalysis, Chem. Eur. J. 18 (2012) 16689–16697, https://doi.org/10.1002/chem.201200499.
[41] R.I. Nooney, D. Thirunavukkarasu, C. Yimei, R. Josephs, A.E. Ostafin, Synthesis of nanoscale mesoporous silica spheres with controlled particle size, Chem. Mater. 14 (2002) 4721–4728, https://doi.org/10.1021/cm0204371.
[42] J. Kecht, T. Bein, Functionalization of colloidal mesoporous silica by metalorganic reagents, Langmuir 24 (2008) 14209–14214, https://doi.org/10.1021/la802115n.
[43] D.G. Choi, S.M. Yang, Effect of two-step sol-gel reaction on the mesoporous silica structure, J. Colloid Interface Sci. 261 (2003) 127–132, https://doi.org/10.1016/S0021-9797(03)00020-1.
[44] G. Villaverde, A. Baeza, G.J. Melen, A. Alfranca, M. Ramirez, M. Vallet-Regí, A new targeting agent for the selective drug delivery of nanocarriers for treating neuroblastoma, J. Mater. Chem. B 3 (2015) 4831–4842, https://doi.org/10.1039/C5TB00287G.
[45] R.R. Castillo, A. Baeza, M. Vallet-Regí, Recent applications of the combination of mesoporous silica nanoparticles with nucleic acids: development of bioresponsive devices, carriers and sensors, Biomater. Sci. 5 (2017) 353–377, https://doi.org/10.1039/C6BM00872K.
[46] M. Vallet-Regí, E. Ruiz-Hernández, B. Gonzalez, A. Baeza, Design of smart nanomaterials for drug and gene delivery, J. Biomater. Tissue Eng. 1 (2011) 6–29, https://doi.org/10.1166/jbt.2011.1006.
[47] Á. Martínez, E. Fuentes-Paniagua, A. Baeza, J. Sánchez-Nieves, M. Cicuéndez, R. Gõmez, et al., Mesoporous silica nanoparticles decorated with carbosilane dendrons as new non-viral oligonucleotide delivery carriers, Chem. Eur. J. 21 (2015) 15651–15666, https://doi.org/10.1002/chem.201501966.
[48] A. Baeza, M. Manzano, M. Colilla, M. Vallet-Regí, Recent advances in mesoporous silica nanoparticles for antitumor therapy: our contribution, Biomater. Sci. 4 (2016) 803–813, https://doi.org/10.1039/C6BM00039H.
[49] V. López, M.R. Villegas, V. Rodríguez, G. Villaverde, D. Lozano, A. Baeza, et al., Janus mesoporous silica nanoparticles for dual targeting of tumor cells and mitochondria, ACS Appl. Mater. Interfaces 9 (2017) 26697–26706, https://doi.org/10.1021/acsami.7b06906.
[50] A. Baeza, Ceramic nanoparticles for cancer treatment, in: Bio-Ceramics with Clin. Appl., 2014, pp. 421–455. doi: 10.1002/9781118406748.ch14.
[51] A. Baeza, D. Ruiz-Molina, M. Vallet-Regí, Recent advances in porous nanoparticles for drug delivery in antitumoral applications: inorganic nanoparticles and nanoscale metal-organic frameworks, Exp. Opin. Drug Deliv. 14 (2017) 783–796, https://doi.org/10.1080/17425247.2016.1229298.
[52] B. Rühle, P. Saint-Cricq, J.I. Zink, Externally controlled nanomachines on mesoporous silica nanoparticles for biomedical applications, ChemPhysChem (2016) 1769–1779, https://doi.org/10.1002/cphc.201501167.
[53] L. Zhang, Y. Chen, Z. Li, L. Li, P. Saint-Cricq, C. Li, et al., Tailored synthesis of octopus-type janus nanoparticles for synergistic actively-targeted and chemo-photothermal therapy, Angew. Chem. Int. Ed. 55 (2016) 2118–2121, https://doi.org/10.1002/anie.201510409.
[54] P. Saint-Cricq, S. Deshayes, J.I. Zink, A.M. Kasko, Magnetic field activated drug delivery using thermodegradable azo-functionalised PEG-coated core–shell mesoporous silica nanoparticles, Nanoscale 7 (2015) 13168–13172, https://doi.org/10.1039/C5NR03777H.
[55] H. Jiang, C. Blouin, Insertions and the emergence of novel protein structure: a structure-based phylogenetic study of insertions, BMC Bioinform. (2007) https://doi.org/10.1186/1471-2105-8-444.
[56] C. Sanchez, F. Ribot, Design of hybrid organic-inorganic materials synthesized via sol-gel chemistry, New J. Chem. 18 (1994) 1007–1047.
[57] C. Sanchez, C. Boissiere, S. Cassaignon, C. Chaneac, O. Durupthy, M. Faustini, et al., Molecular engineering of functional inorganic and hybrid materials, Chem. Mater. 26 (2014) 221–238, https://doi.org/10.1021/cm402528b.
[58] N. Baccile, G. Laurent, T. Azaïs, F. Babonneau, NMR characterisation of the organic/SiO2 interfaces in templated porous silica, Mater. Res. Soc. Symp. Proc. 984 (2007) 984-NaN-6.
[59] F. Babonneau V. Gualandris M. Pauthe, NMR Characterization of the Chemical Homogeneity in Sol-Gel Derived Siloxane-Silica Materials, 1996.
[60] C. Bonhomme, C. Coelho, N. Baccile, C. Gervais, T. Azaïs, F. Babonneau, Advanced solid state NMR techniques for the characterization of sol – gel-derived materials, Acc. Chem. Res. 738–746 (2007).
[61] H. Djojoputro, X.F. Zhou, S.Z. Qiao, L.Z. Wang, C.Z. Yu, G.Q. Lu, Periodic mesoporous organosilica hollow spheres with tunable wall thickness, J. Am. Chem. Soc. 128 (2006) 6320–6321, https://doi.org/10.1021/ja0607537.
[62] B. Guan, Y. Cui, Z. Ren, Z. Qiao, L. Wang, Y. Liu, et al., Highly ordered periodic mesoporous organosilica nanoparticles with controllable pore structures, Nanoscale 4 (2012) 6588, https://doi.org/10.1039/c2nr31662e.
[63] S. Parambadath, A. Mathew, M.J. Barnabas, K.M. Rao, C.S. Ha, Periodic mesoporous organosilica (PMO) containing bridged succinamic acid groups as a nanocarrier for sulfamerazine, sulfadiazine and famotidine: Adsorption and release study, Microporous Mesoporous Mater. 225 (2016) 174–184, https://doi.org/10.1016/j.micromeso.2015.12.016.
[64] Z. Teng, X. Su, Y. Zheng, J. Zhang, Y. Liu, S. Wang, et al., A facile multi-interface transformation approach to monodisperse multiple-shelled periodic mesoporous organosilica hollow spheres, J. Am. Chem. Soc. 137 (2015) 7935–7944, https://doi.org/10.1021/jacs.5b05369.
[65] P. Van Der Voort, D. Esquivel, E. De Canck, F. Goethals, I. Van Driessche, F.J. Romero-Salguero, Periodic Mesoporous Organosilicas: from simple to complex bridges; a comprehensive overview of functions, morphologies and applications, Chem. Soc. Rev. 42 (2013) 3913–3955, https://doi.org/10.1039/C2CS35222B.
[66] D. Lu, J. Lei, L. Wang, J. Zhang, Multifluorescently traceable nanoparticle by a single-wavelength excitation with color-related drug release performance, J. Am. Chem. Soc. 134 (2012) 8746–8749, https://doi.org/10.1021/ja301691j.
[67] R. Kumar, I. Roy, T. Ohulchanskky, L. Vathy, E.J. Bergey, M. Sajjad, et al., In vivo biodistribution and clearance studies using multimodal organically modified silica nanoparticles, ACS Nano 4 (2010) 699–708, https://doi.org/10.1021/nn901146y.In.
[68] Y. Chen, J. Shi, Chemistry of mesoporous organosilica in nanotechnology: molecularly organic-inorganic hybridization into frameworks, Adv. Mater. 28 (2016) 3235–3272, https://doi.org/10.1002/adma.201505147.
[69] T. Yanagisawa, T. Shimizu, K. Kuroda, C. Kato, The preparation of alkyltrimethylammonium-kanemite complexes and their conversion to microporous materials, Bull. Chem. Soc. Jpn. 63 (1990) 988–992, https://doi.org/10.1246/bcsj.63.988.
[70] C.T. Kresge, M.E. Leonowicz, W.J. Roth, J.C. Vartuli, J.S. Beck, Ordered mesoporous molecular sieves synthesized by a liquid-crystal template mechanism, Nature 359 (1992) 710, https://doi.org/10.1038/359710a0.
[71] J.S. Beck, J.C. Vartuli, W.J. Roth, M.E. Leonowicz, C.T. Kresge, et al., A new family of mesoporous molecular sieves prepared with liquid crystal templates, 10384 J. Am. Chem. Soc. 14 (1992) https://doi.org/10.1021/ja00053a020.
[72] S. Inagaki, S. Guan, Y. Fukushima, T. Ohsuna, O. Terasaki, Novel mesoporous materials with a uniform distribution of organic groups and inorganic oxide in their frameworks, J. Am. Chem. Soc. 121 (1999) 9611–9614, https://doi.org/10.1021/ja9916658.
[73] T. Asefa, M.J. MacLachan, N. Coombs, G.A. Ozin, Periodic mesoporous organosilicas with organic groups inside the channel walls, Nature 402 (1999) 867–871, https://doi.org/10.1038/47229.
[74] B.J. Melde, B.T. Holland, C.F. Blanford, A. Stein, Mesoporous sieves with unified hybrid inorganic/organic frameworks, Chem. Mater. 11 (1999) 3302–3308, https://doi.org/10.1021/cm9903935.

[75] Y. Lu, H. Fan, A. Stump, T.L. Ward, T. Rieker, C.J. Brinker, Aerosol-assisted self-assembly of mesostructured spherical nanoparticles, Nature 398 (1999) 223–226, https://doi.org/10.1038/18410.
[76] C.J. Brinker, Y. Lu, A. Sellinger, H. Fan, Evaporation-induced self-assembly: nanostructures made easy, Adv. Mater. 11 (1999) 579–585, https://doi.org/10.1002/(SICI)1521-4095(199905)11:7<579::AID-ADMA579>3.0.CO;2-R.
[77] Y. Lu, H. Fan, N. Doke, D.A. Loy, R.A. Assink, D.A. LaVan, et al., Evaporation-induced self-assembly of hybrid bridged silsesquioxane film and particulate mesophases with integral organic functionality, J. Am. Chem. Soc. 122 (2000) 5258–5261, https://doi.org/10.1021/ja9935862.
[78] K.J. Shea, D.A. Loy, Bridged polysilsesquioxanes. Molecular-engineered hybrid organic-inorganic materials, Chem. Mater. 13 (2001) 3306–3319, https://doi.org/10.1021/cm011074s.
[79] K.J. Shea, D.A. Loy, A mechanistic investigation of gelation. The sol-gel polymerization of precursors to bridged polysilsesquioxanes, Acc. Chem. Res. 34 (2001) 707–716, https://doi.org/10.1021/ar000109b.
[80] G. Creff, B.P. Pichon, C. Blanc, D. Maurin, J.L. Sauvajol, C. Carcel, et al., Self-assembly of bridged silsesquioxanes: Modulating structural evolution via cooperative covalent and noncovalent interactions, Langmuir 29 (2013) 5581–5588, https://doi.org/10.1021/la400293k.
[81] A. Monge-Marcet, X. Cattoën, P. Dieudonné, R. Pleixats, M. Wong Chi Man, Nanostructuring of ionic bridged silsesquioxanes, Chem. Asian J. 8 (2013) 2235–2241, https://doi.org/10.1002/asia.201300538.
[82] G. Creff, G. Arrachart, P. Hermet, H. Wadepohl, R. Almairac, D. Maurin, et al., Investigation on the vibrational and structural properties of a self-structured bridged silsesquioxane, Phys. Chem. Chem. Phys. 14 (2012) 5672, https://doi.org/10.1039/c2cp40250e.
[83] G. Arrachart, G. Creff, H. Wadepohl, C. Blanc, C. Bonhomme, F. Babonneau, et al., Nanostructuring of hybrid silicas through a self-recognition process, Chem. Eur. J. 15 (2009) 5002–5005, https://doi.org/10.1002/chem.200802748.
[84] P. Dieudonné, M.W.C. Man, B.P. Pichón, L. Vellutini, J.L. Bantignies, C. Blanc, et al., In situ X-ray measurements to probe a new solid-state polycondensation mechanism for the design of supramolecular organo-bridged silsesquioxanes, Small 5 (2009) 503–510, https://doi.org/10.1002/smll.200800254.
[85] J.J.E. Moreau, B.P. Pichon, C. Bied, M.W.C. Man, Structuring of bridged silsesquioxanes via cooperative weak interactions: H-bonding of urea groups and hydrophobic interactions of long alkylene chains, J. Mater. Chem. 15 (2005) 3929–3936, https://doi.org/10.1039/b504635a.
[86] J.J.E. Moreau, L. Vellutini, M.W.C. Man, C. Bied, P. Dieudonné, J.L. Bantignies, et al., Lamellar bridged silsesquioxanes: Self-assembly through a combination of hydrogen bonding and hydrophobic interactions, Chem. Eur. J. 11 (2005) 1527–1537, https://doi.org/10.1002/chem.200401012.
[87] J.J.E. Moreau, L. Vellutini, M.W.C. Man, C. Bied, J.L. Bantignies, P. Dieudonné, et al., Self-organized hybrid silica with long-range ordered lamellar structure, J. Am. Chem. Soc. 123 (2001) 7957–7958, https://doi.org/10.1021/ja016053d.
[88] J.L. Bantignies, L. Vellutini, D. Maurin, P. Hermet, P. Dieudonné, M.W.C. Man, et al., Insights into the self-directed structuring of hybrid organic – inorganic silicas through infrared studies, J. Phys. Chem. B 110 (2006) 15797–15802, https://doi.org/10.1021/jp060975r.
[89] J.J.E. Moreau, B.P. Pichon, M. Wong Chi Man, C. Bied, H. Pritzkow, J.L. Bantignies, et al., A better understanding of the self-structuration of bridged silsesquioxanes, Angew. Chem. Int. Ed. 43 (2003) 203–206, https://doi.org/10.1002/anie.200352485.
[90] A. Monge-Marcet, X. Cattoën, D.A. Alonso, C. Nájera, M.W.C. Man, R. Pleixats, Recyclable silica-supported prolinamide organocatalysts for direct asymmetric Aldol reaction in water, Green Chem. 14 (2012) 1601, https://doi.org/10.1039/c2gc35227c.
[91] M. Ferré, R. Pleixats, M. Wong Chi Man, X. Cattoën, Recyclable organocatalysts based on hybrid silicas, Green Chem. 18 (2016) 881–922, https://doi.org/10.1039/C5GC02579F.
[92] Y. Maegawa, S. Inagaki, Iridium–bipyridine periodic mesoporous organosilica catalyzed direct C-H borylation using a pinacolborane, Dalton Trans. 44 (2015) 13007–13016, https://doi.org/10.1039/C5DT00239G.
[93] M. Ohashi, M. Aoki, K.I. Yamanaka, K. Nakajima, T. Ohsuna, T. Tani, et al., A periodic mesoporous organosilica-based donor-acceptor system for photocatalytic hydrogen evolution, Chem. Eur. J. 15 (2009) 13041–13046, https://doi.org/10.1002/chem.200901721.
[94] H. Takeda, M. Ohashi, T. Tani, O. Ishitani, S. Inagaki, Enhanced photocatalysis of rhenium(I) complex by light-harvesting periodic mesoporous organosilica, Inorg. Chem. 49 (2010) 4554–4559, https://doi.org/10.1021/ic1000914.
[95] X. Liu, Y. Maegawa, Y. Goto, K. Hara, S. Inagaki, Heterogeneous catalysis for water oxidation by an iridium complex immobilized on bipyridine-periodic mesoporous organosilica, Angew. Chem. Int. Ed. 55 (2016) 7943–7947, https://doi.org/10.1002/anie.201601453.
[96] J.J.E. Moreau, M.W.C. Man, The design of selective catalysts from hybrid silica-based materials, Coord. Chem. Rev. 178 (1998) 1073–1084, https://doi.org/10.1016/S0010-8545(98)00156-8.
[97] A. Zamboulis, N. Moitra, J.J.E. Moreau, X. Cattoën, M. Wong Chi Man, Hybrid materials: versatile matrices for supporting homogeneous catalysts, J. Mater. Chem. 20 (2010) 9322, https://doi.org/10.1039/c000334d.
[98] J.Y. Shi, C.A. Wang, Z.J. Li, Q. Wang, Y. Zhang, W. Wang, Heterogeneous organocatalysis at work: functionalization of hollow periodic mesoporous organosilica spheres with MacMillan catalyst, Chem. Eur. J. 17 (2011) 6206–6213, https://doi.org/10.1002/chem.201100072.
[99] S.S. Park, M.S. Moorthy, C.-S. Ha, Periodic mesoporous organosilica (PMO) for catalytic applications, Korean J. Chem. Eng. 31 (2014) 1707–1719, https://doi.org/10.1007/s11814-014-0221-1.
[100] D. Esquivel, C. Jiménez-Sanchidrián, F.J. Romero-Salguero, Thermal behaviour, sulfonation and catalytic activity of phenylene-bridged periodic mesoporous organosilicas, J. Mater. Chem. 21 (2011) 724, https://doi.org/10.1039/c0jm02980g.
[101] D. Esquivel, E. De Canck, C. Jiménez-Sanchidrián, P. Van Der Voort, F.J. Romero-Salguero, Formation and functionalization of surface Diels-Alder adducts on ethenylene-bridged periodic mesoporous organosilica, J. Mater. Chem. 21 (2011) 10990, https://doi.org/10.1039/c1jm11315a.
[102] V.T. Freitas, L. Fu, A.M. Cojocariu, X. Cattoën, J.R. Bartlett, R. Le Parc, et al., Eu^{3+}-based bridged silsesquioxanes for transparent luminescent solar concentrators, ACS Appl. Mater. Interfaces 7 (2015) 8770–8778, https://doi.org/10.1021/acsami.5b01281.
[103] H. Takeda, Y. Goto, Y. Maegawa, T. Ohsuna, T. Tani, K. Matsumoto, et al., Visible-light-harvesting periodic mesoporous organosilica, Chem. Commun. 6032 (2009) https://doi.org/10.1039/b910528j.
[104] S. Inagaki, O. Ohtani, Y. Goto, K. Okamoto, M. Ikai, K.I. Yamanaka, et al., Light harvesting by a periodic mesoporous organosilica chromophore, Angew. Chem. Int. Ed. 48 (2009) 4042–4046, https://doi.org/10.1002/anie.200900266.
[105] M. Ikai, Y. Maegawa, Y. Goto, T. Tani, S. Inagaki, Synthesis of visible-light-absorptive and hole-transporting periodic mesoporous organosilica thin films for organic solar cells, J. Mater. Chem. A 2 (2014) 11857–11865, https://doi.org/10.1039/C4TA01136H.
[106] Y. Yamamoto, H. Takeda, T. Yui, Y. Ueda, K. Koike, S. Inagaki, et al., Efficient light harvesting via sequential two-step energy accumulation using a Ru-Re5 multinuclear complex incorporated into periodic mesoporous organosilica, Chem. Sci. 5 (2014) 639–648, https://doi.org/10.1039/c3sc51959g.
[107] J. Graffion, A.M. Cojocariu, X. Cattoën, R.A.S. Ferreira, V.R. Fernandes, P.S. André, et al., Luminescent coatings from bipyridine-based bridged silsesquioxanes containing Eu3+ and Tb3+ salts, J. Mater. Chem. 22 (2012) 13279, https://doi.org/10.1039/c2jm31289a.
[108] M. Fernandes, R.A.S. Ferreira, X. Cattoën, L.D. Carlos, M. Wong Chi Man, V. De, Zea Bermudez, Photoluminescent lamellar bilayer mono-alkyl-urethanesils, J. Sol-Gel Sci. Technol. 65 (2013) 61–73, https://doi.org/10.1007/s10971-012-2739-1.
[109] J. Graffion, X. Cattoën, V.T. Freitas, R.A.S. Ferreira, M.W. Chi Man, L.D. Carlos, Engineering of metal-free bipyridine-based bridged silsesquioxanes for sustainable solid-state lighting, J. Mater. Chem. 22 (2012) 6711, https://doi.org/10.1039/c2jm15225h.
[110] J. Graffion, X. Cattoën, M. Wong Chi Man, V.R. Fernandes, P.S. André, R.A.S. Ferreira, et al., Modulating the photoluminescence of bridged silsesquioxanes incorporating Eu3+-complexed n, n′-diureido-2,2′-bipyridine isomers: application for luminescent solar concentrators, Chem. Mater. 23 (2011) 4773–4782, https://doi.org/10.1021/cm2019026.
[111] S.S. Nobre, X. Cattoën, R.A.S. Ferreira, C. Carcel, V. De Zea Bermudez, M. Wong Chi Man, et al., Eu3+-Assisted short-range ordering of photoluminescent bridged silsesquioxanes, Chem. Mater. 22 (2010) 3599–3609, https://doi.org/10.1021/cm1009042.
[112] T. Tani, N. Mizoshita, S. Inagaki, Luminescent periodic mesoporous organosilicas, J. Mater. Chem. 19 (2009) 4451, https://doi.org/10.1039/b820691k.
[113] A. Noureddine, P. Trens, G. Toquer, X. Cattoën, M.W. Ong, C. Man, Tailoring the hydrophilic/lipophilic balance of clickable mesoporous organosilicas by the copper-catalyzed azide-alkyne cycloaddition click-functionalization, Langmuir 30 (2014) 12297–12305, https://doi.org/10.1021/la503151w.
[114] E. Besson, A. Mehdi, A. Van Der Lee, H. Chollet, C. Reyé, R. Guilard, et al., Selective lanthanides sequestration based on a self-assembled organosilica, Chem. Eur. J. 16 (2010) 10226–10233, https://doi.org/10.1002/chem.200902454.
[115] D. Hérault, G. Cerveau, R.J.P. Corriu, A. Mehdi, New mesostructured organosilica with chiral sugar derived structures: nice host for gold nanoparticles stabilisation, Dalton Trans. 40 (2011) 446–451, https://doi.org/10.1039/c0dt01162b.
[116] R.J.P. Corriu, E. Lancelle-Beltran, A. Mehdi, C. Reyé, S. Brandès, R. Guilard, Ordered mesoporous hybrid materials containing cobalt(ii) Schiff base complex, J. Mater. Chem. 12 (2002) 1355–1362, https://doi.org/10.1039/b200478j.
[117] Y.T. Prabhu, K.V. Rao, B.S. Kumari, V.S.S. Kumar, T. Pavani, Synthesis of Fe3O4 nanoparticles and its antibacterial application, Int. Nano Lett. 5 (2015) 85–92, https://doi.org/10.1007/s40089-015-0141-z.
[118] Ö. Dag, C. Yoshina-Ishii, T. Asefa, M.J. MacLachlan, H. Grondey, N. Coombs, et al., Oriented periodic mesoporous organosilica (PMO) film with organic functionality inside the channel walls, Adv. Funct. Mater. 11 (2001) 213–217, https://doi.org/10.1002/1616-3028(200106)11:3<213::AID-ADFM213>3.0.CO;2-C.
[119] B.D. Hatton, K. Landskron, W. Whitnall, D.D. Perovic, G.A. Ozin, Spin-coated periodic mesoporous organosilica thin films – towards a new generation of low-dielectric-constant materials, Adv. Funct. Mater. 15 (2005) 823–829, https://doi.org/10.1002/adfm.200400221.
[120] N. Mizoshita, M. Ikai, T. Tani, S. Inagaki, Hole-transporting periodic mesostructured organosilica, J. Am. Chem. Soc. 131 (2009) 14225–14227, https://doi.org/10.1021/ja9050263.
[121] B. Camareta, B. Onida, Y. Goto, S. Inagaki, E. Garrone, Hydroxyl species in large-pore phenylene-bridged periodic mesoporous organosilica, Langmuir 23 (2007) 13164–13168, https://doi.org/10.1021/la702252j.
[122] B. Camarota, Y. Goto, S. Inagaki, B. Onida, Basic sites on periodic mesoporous organosilicas investigated by XPS and in situ FTIR of adsorbed pyrrole, Langmuir 27 (2011) 1181–1185, https://doi.org/10.1021/la103814w.
[123] B. Camarota, Y. Goto, S. Inagaki, E. Garrone, B. Onida, Electron-rich sites at the surface of periodic mesoporous organosilicas: a UV-visible characterization of adsorbed iodine, J. Phys. Chem. C. 113 (2009) 20396–20400, https://doi.org/10.1021/jp906696f.
[124] B. Ameduri, B. Boutevin, J.J. Moreau, H. Moutaabbid, M. Wong Chi Man, Hybrid organic–inorganic gels containing perfluoro-alkyl moieties, J. Fluor. Chem. 104 (2000) 185–194, https://doi.org/10.1016/S0022-1139(00)00211-6.
[125] J.J.E. Moreau, L. Vellutini, C. Wong Chi Man, C. Bied, New hybrid organic-inorganic solids with helical morphology via H-bond mediated sol-gel hydrolysis of

silyl derivatives of chiral (R,R)- or (S,S)-diureidocyclohexane [6], J. Am. Chem. Soc. 123 (2001) 1509–1510, https://doi.org/10.1021/ja003843z.
[126] K. Bürglová, A. Noureddine, J. Hodačová, G. Toquer, X. Cattoën, M. Wongchiman, A general method for preparing bridged organosilanes with pendant functional groups and functional mesoporous organosilicas, Chem. Eur. J. 20 (2014) 10371–10382, https://doi.org/10.1002/chem.201403136.
[127] D. Esquivel, O. van den Berg, F.J. Romero-Salguero, F. Du Prez, P. Van der Voort, 100% thiol-functionalized ethylene PMOs prepared by "thiol acid-ene" chemistry, Chem. Commun. 49 (2013) 2344–2346, https://doi.org/10.1039/c3cc39074h.
[128] W.J. Hunks, G.A. Ozin, Periodic mesoporous organosilicas with phenylene bridging groups, 1,4-(CH2)nC6H4 (n = 0–2), Chem. Mater. 16 (2004) 5465–5472, https://doi.org/10.1021/cm048986p.
[129] T. Asefa, M. Kruk, N. Coombs, H. Grondey, M.J. MacLachlan, M. Jaroniec, et al., Novel route to periodic mesoporous aminosilicas, PMAs: ammonolysis of periodic mesoporous organosilicas, J. Am. Chem. Soc. 125 (2003) 11662–11673, https://doi.org/10.1021/ja036080z.
[130] W.J. Hunks, G.A. Ozin, Engineering porosity in bifunctional periodic mesoporous organosilicas with MT- and DT-type silica building blocks, J. Mater. Chem. 15 (2005) 764–771, https://doi.org/10.1039/b412963f.
[131] T. Asefa, M. Kruk, M.J. MacLachlan, N. Coombs, H. Grondey, M. Jaroniec, et al., Novel bifunctional periodic mesoporous organosilicas, BPMOs: synthesis, characterization, properties and in-situ selective hydroboration – alcoholysis reactions of functional groups, J. Am. Chem. Soc. 123 (2001) 8520–8530, https://doi.org/10.1021/ja0037320.
[132] J.R. Matos, M. Kruk, L.P. Mercuri, M. Jaroniec, T. Asefa, N. Coombs, et al., Periodic mesoporous organosilica with large cagelike pores, Chem. Mater. 14 (2002) 1903–1905, https://doi.org/10.1021/cm025513e.
[133] S. Inagaki, S. Guan, T. Ohsuna, O. Terasaki, An ordered mesoporous organosilica hybrid material with a crystal-like wall structure, Nature 416 (2002) 304–307, https://doi.org/10.1038/416304a.
[134] M. Waki, N. Mizoshita, T. Ohsuna, T. Tani, S. Inagaki, Crystal-like periodic mesoporous organosilica bearing pyridine units within the framework, Chem. Commun. 46 (2010) 8163, https://doi.org/10.1039/c0cc01944e.
[135] N. Mizoshita, S. Inagaki, Periodic mesoporous organosilica with molecular-scale ordering self-assembled by hydrogen bonds, Angew. Chem. Int. Ed. 54 (2015) 11999–12003, https://doi.org/10.1002/anie.201505538.
[136] N. Mizoshita, T. Tani, H. Shinokubo, S. Inagaki, Mesoporous organosilica hybrids consisting of silica-wrapped π-π stacking columns, Angew. Chem. Int. Ed. 51 (2012) 1156–1160, https://doi.org/10.1002/anie.201105394.
[137] R.J.P. Corriu, D. Leclercq, Recent developments of molecular chemistry for sol-gel processes, Angew. Chem. Int. Ed. Engl. 35 (1996) 1420–1436, https://doi.org/10.1002/anie.199614201.
[138] N. Bellec, F. Lerouge, B. Pichon, G. Cerveau, R.J.P. Corriu, D. Lorcy, (Trialkoxysilyl)tetrathiafulvalenes: Precursors of organized organic-inorganic hybrid materials by sol-gel chemistry, Eur. J. Org. Chem. (2004) 136–146, https://doi.org/10.1002/ejoc.200400485.
[139] R.J.P. Corriu, Ceramics and nanostructures from molecular precursors, Angew. Chem. Int. Ed. 39 (2000) 1376–1398, https://doi.org/10.1002/(SICI)1521-3773(20000417)39:8<1376::AID-ANIE1376>3.0.CO;2-S.
[140] W.J. Hunks, G.A. Ozin, Single-source precursors for synthesizing bifunctional periodic mesoporous organosilicas, Adv. Funct. Mater. 15 (2005) 259–266, https://doi.org/10.1002/adfm.200400294.
[141] W. Whitnall, T. Asefa, G.A. Ozin, Hybrid periodic mesoporous organosilicas, Adv. Funct. Mater. 15 (2005) 1696–1702, https://doi.org/10.1002/adfm.200500151.
[142] B. Hatton, K. Landskron, W. Whitnall, D. Perovic, G.A. Ozin, Past, present, and future of periodic mesoporous organosilicas – the PMOs, Acc. Chem. Res. 38 (2005) 305–312, https://doi.org/10.1021/ar040164a.
[143] W.J. Hunks, G.A. Ozin, Challenges and advances in the chemistry of periodic mesoporous organosilicas (PMOs), J. Mater. Chem. 15 (2005) 3716, https://doi.org/10.1039/b504511h.
[144] M. Waki, N. Mizoshita, T. Tani, S. Inagaki, Periodic mesoporous organosilica derivatives bearing a high density of metal complexes on pore surfaces, Angew. Chem. Int. Ed. 50 (2011) 11667–11671, https://doi.org/10.1002/anie.201104063.
[145] B. Camarota, P. Ugliengo, E. Garrone, C.O. Arean, M.R. Delgado, S. Inagaki, et al., IR and computational characterization of CO adsorption on a model surface, the phenylene periodic mesoporous organosilica with crystalline walls, J. Phys. Chem. C 112 (2008) 19560–19567, https://doi.org/10.1021/jp805981a.
[146] Y. Li, A. Keilbach, M. Kienle, Y. Goto, S. Inagaki, P. Knochel, et al., Hierarchically structured biphenylene-bridged periodic mesoporous organosilica, J. Mater. Chem. 21 (2011) 17338, https://doi.org/10.1039/c1jm12023a.
[147] N. Tanaka, N. Mizoshita, Y. Maegawa, T. Tani, S. Inagaki, Y.R. Jorapur, et al., Synthesis of a spirobifluorene-bridged allylsilane precursor for periodic mesoporous organosilica, Chem. Commun. 47 (2011) 5025, https://doi.org/10.1039/c0cc05823h.
[148] T. Okada, K. Yamanaka, Y. Hirose, Y. Goto, T. Tani, S. Inagaki, Fluorescence studies on phenylene moieties embedded in a framework of periodic mesoporous organosilica, Phys. Chem. Chem. Phys. 13 (2011) 7961–7967, https://doi.org/10.1039/c0cp02714f.
[149] Y. Li, A. Keilbach, N. Mizoshita, S. Inagaki, T. Bein, Formation of hexagonal and cubic fluorescent periodic mesoporous organosilicas in the channels of anodic alumina membranes, J. Mater. Chem. C 2 (2014) 50, https://doi.org/10.1039/c3tc00008g.
[150] N. Mizoshita, T. Tani, S. Inagaki, Syntheses, properties and applications of periodic mesoporous organosilicas prepared from bridged organosilane precursors, Chem. Soc. Rev. 40 (2011) 789–800, https://doi.org/10.1039/C0CS00010H.
[151] M. Waki, Y. Maegawa, K. Hara, Y. Goto, S. Shirai, Y. Yamada, et al., A solid chelating ligand: periodic mesoporous organosilica containing 2,2′-bipyridine within the pore walls, J. Am. Chem. Soc. 136 (2014) 4003–4011, https://doi.org/10.1021/ja4131609.
[152] K. Yamanaka, T. Okada, Y. Goto, T. Tani, S. Inagaki, Exciton migration dynamics between phenylene moieties in the framework of periodic mesoporous organosilica powder, RSC Adv. 3 (2013) 14774, https://doi.org/10.1039/c3ra41619d.
[153] T. Yui, H. Takeda, Y. Ueda, K. Sekizawa, K. Koike, S. Inagaki, et al., Hybridization between periodic mesoporous organosilica and a Ru(II) polypyridyl complex with phosphonic acid anchor groups, ACS Appl. Mater. Interfaces 6 (2014) 1992–1998, https://doi.org/10.1021/am405065a.
[154] K.I. Yamanaka, T. Okada, Y. Goto, M. Ikai, T. Tani, S. Inagaki, Dynamics of excitation energy transfer from biphenylylene excimers in pore walls of periodic mesoporous organosilica to coumarin 1 in the mesochannels, J. Phys. Chem. C 117 (2013) 14865–14871, https://doi.org/10.1021/jp404691c.
[155] M. Mandal, M. Kruk, Large-pore ethylene-bridged periodic mesoporous organosilicas with face-centered cubic structure, J. Phys. Chem. C 114 (2010) 20091–20099, https://doi.org/10.1021/jp1069187.
[156] V. Rebbin, A. Rothkirch, N. Ohta, T. Hikima, S.S. Funari, Size limit on the formation of periodic mesoporous organosilicas (PMOs), Langmuir 30 (2014) 1900–1905, https://doi.org/10.1021/la404060a.
[157] S. Masse, G. Laurent, F. Babonneau, High temperature behavior of periodic mesoporous ethanesilica glasses prepared from a bridged silsesquioxane and a non-ionic triblock copolymer, J. Non Cryst. Solids 353 (2007) 1109–1119, https://doi.org/10.1016/j.jnoncrysol.2006.12.020.
[158] N.M. El-Ashgar, M.K. Silmi, I.M. El-Nahhal, M.M. Chehimi, F. Babonneau, Template synthesis of iminodiacetic acid polysiloxane immobilized ligand systems and their metal uptake capacity, Silicon 9 (2017) 563–575, https://doi.org/10.1007/s12633-015-9303-x.
[159] L. Zhao, D.A. Loy, K.J. Shea, Photodeformable spherical hybrid nanoparticles, J. Am. Chem. Soc. 128 (2006) 14250–14251, https://doi.org/10.1021/ja066047n.
[160] L. Yang, L. Wang, C. Cui, J. Lei, J. Zhang, Stöber strategy for synthesizing multifluorescent organosilica nanocrystals, Chem. Commun. 52 (2016) 6154–6157, https://doi.org/10.1039/C6CC01917J.
[161] M. Nakamura, K. Ishimura, One-pot synthesis and characterization of three kinds of thiol – organosilica nanoparticles, Langmuir 24 (2008) 5099–5108, https://doi.org/10.1021/la703395w.
[162] M. Nakamura, K. Ishimura, Synthesis and characterization of organosilica nanoparticles prepared from 3-mercaptopropyltrimethoxysilane as the single silica source, J. Phys. Chem. C 111 (2007) 18892–18898, https://doi.org/10.1021/jp075798o.
[163] A. Arkhireeva, J.N. Hay, W. Oware, A versatile route to silsesquioxane nanoparticles from organically modified silane precursors, J. Non Cryst. Solids 351 (2005) 1688–1695, https://doi.org/10.1016/j.jnoncrysol.2005.04.063.
[164] A. Arkhireeva, J.N. Hay, J.M. Lane, M. Manzano, H. Masters, W. Oware, et al., Synthesis of organic-inorganic hybrid particles by sol-gel chemistry, J. Sol-Gel Sci. Technol. 31 (2004) 31–36, https://doi.org/10.1023/B:JSST.0000047956.24117.89.
[165] A. Arkhireeva, J.N. Hay, Synthesis of sub-200 nm silsesquioxane particles using a modified Stöber sol–gel route, J. Mater. Chem. 13 (2003) 3122–3127, https://doi.org/10.1039/B306994J.
[166] M. Nakamura, K. Hayashi, M. Nakano, T. Kanadani, K. Miyamoto, T. Kori, et al., Identification of polyethylene glycol-resistant macrophages on stealth imaging in vitro using fluorescent organosilica nanoparticles, ACS Nano 9 (2015) 1058–1071, https://doi.org/10.1021/nn502319r.
[167] X. Ma, J. Zhang, M. Dang, J. Wang, Z. Tu, L. Yuwen, et al., Hollow periodic mesoporous organosilica nanospheres by a facile emulsion approach, J. Colloid Interface Sci. 475 (2016) 66–71, https://doi.org/10.1016/j.jcis.2016.04.026.
[168] Y. Chen, Q. Meng, M. Wu, S. Wang, P. Xu, H. Chen, et al., Hollow mesoporous organosilica nanoparticles: a generic intelligent framework-hybridization approach for biomedicine, J. Am. Chem. Soc. 136 (2014) 16326–16334, https://doi.org/10.1021/ja508721y.
[169] Y. Xing, J. Peng, K. Xu, W. Lin, S. Gao, Y. Ren, et al., Polymerizable molecular silsesquioxane cage armored hybrid microcapsules with in situ shell functionalization, Chem. Eur. J. 22 (2016) 2114–2126, https://doi.org/10.1002/chem.201504473.
[170] F. Dong, W. Guo, S.-K. Park, C.-S. Ha, Controlled synthesis of novel cyanopropyl polysilsesquioxane hollow spheres loaded with highly dispersed Au nanoparticles for catalytic applications, Chem. Commun. 48 (2012) 1108–1110, https://doi.org/10.1039/C1CC14831A.
[171] Q. Wang, Y. Liu, H. Yan, Mechanism of a self-templating synthesis of monodispersed hollow silica nanospheres with tunable size and shell thickness, Chem. Commun. (2007) 2339–2341, https://doi.org/10.1039/b701572k.
[172] L. Maggini, L. Travaglini, I. Cabrera, P. Castro-Hartmann, L. De Cola, Biodegradable peptide-silica nanodonuts, Chem. Eur. J. 22 (2016) 3697–3703, https://doi.org/10.1002/chem.201504605.
[173] B.P. Pichon, M.W.C. Man, P. Dieudonné, J.L. Bantignies, C. Bied, J.L. Sauvajol, et al., Size and shape dependence of organo-interconnected silsesquioxanes through hydrolysis-condensation reaction conditions: nanotubes, spheres and films, Adv. Funct. Mater. 17 (2007) 2349–2355, https://doi.org/10.1002/adfm.200600670.
[174] J.J.E. Moreau, L. Vellutini, M.W. Chi Man, C. Bied, Shape-controlled bridged silsesquioxanes: hollow tubes and spheres, Chem. Eur. J. 9 (2003) 1594–1599, https://doi.org/10.1002/chem.200390183.
[175] Y. Yang, M. Nakazawa, M. Suzuki, M. Kimura, H. Shirai, K. Hanabusa, Formation of helical hybrid silica bundles, Chem. Mater. 16 (2004) 3791–3793, https://doi.org/10.1021/cm0489993.
[176] V. Čaplar, M. Žinić, J.L. Pozzo, F. Fages, G. Mieden-Gundert, F. Vögtle, Chiral gelators constructed from 11-aminoundecanoic (AUDA), lauric and amino acid units. synthesis, gelling properties and preferred gelation of racemates vs. the pure enantiomers, Eur. J. Org. Chem. (2004) 4048–4059, https://doi.org/10.1002/ejoc.200400105.

[177] P. Mohanty, K. Landskron, Simple systematic synthesis of periodic mesoporous organosilica nanoparticles with adjustable aspect ratios, Nanoscale Res. Lett. 4 (2009) 1524–1529, https://doi.org/10.1007/s11671-009-9430-7.
[178] P. Yuan, L. Zhao, N. Liu, G. Wei, Y. Zhang, Y. Wang, et al., Periodic mesoporous organosilicas with helical and concentric circular pore architectures, Chem. Eur. J. 15 (2009) 11319–11325, https://doi.org/10.1002/chem.200802716.
[179] J. Croissant, X. Cattoën, M. Wong Chi Man, P. Dieudonné, C. Charnay, L. Raehm, et al., One-pot construction of multipodal hybrid periodic mesoporous organosilica nanoparticles with crystal-like architectures, Adv. Mater. 27 (2015) 145–149, https://doi.org/10.1002/adma.201404226.
[180] Z. Teng, C. Wang, Y. Tang, W. Li, L. Bao, X. Zhang, et al., Deformable hollow periodic mesoporous organosilica nanocapsules for significantly improved cellular uptake, J. Am. Chem. Soc. (2017) https://doi.org/10.1021/jacs.7b10694, jacs.7b10694.
[181] J. Croissant, M. Maynadier, O. Mongin, V. Hugues, M. Blanchard-Desce, A. Chaix, et al., Enhanced two-photon fluorescence imaging and therapy of cancer cells via Gold@Bridged silsesquioxane nanoparticles, Small 11 (2015) 295–299, https://doi.org/10.1002/smll.201401759.
[182] M. Faisal, Y. Hong, J. Liu, Y. Yu, J.W.Y. Lam, A. Qin, et al., Fabrication of fluorescent silica nanoparticles hybridized with AIE luminogens and exploration of their applications as nanobiosensors in intracellular imaging, Chem. Eur. J. 16 (2010) 4266–4272, https://doi.org/10.1002/chem.200901823.
[183] C.M. Jimenez, N.Z. Knezevic, Y.G. Rubio, S. Szunerits, R. Boukherroub, F. Teodorescu, et al., Nanodiamond–PMO for two-photon PDT and drug delivery, J. Mater. Chem. B 4 (2016) 5803–5808, https://doi.org/10.1039/C6TB01915C.
[184] X. Wang, B. Guan, Y. He, D. An, Y. Zhang, Y. Cao, et al., Megranate-like nanoreactor with multiple cores and an acidic mesoporous shell for a cascade reaction, Nanoscale (2015) 3719–3725, https://doi.org/10.1039/c4nr06341d.
[185] D. Chen, N. Li, F. Tang, S. Qi, Facile and scalable synthesis of tailored silica "nanorattle" structures, Adv. Mater. 21 (2009) 3804–3807, https://doi.org/10.1002/adma.200900599.
[186] J.G. Croissant, X. Cattoën, M. Wong Chi Man, J.-O. Durand, N.M. Khashab, Syntheses and applications of periodic mesoporous organosilica nanoparticles, Nanoscale 7 (2015) 20318–20334, https://doi.org/10.1039/C5NR05649G.
[187] J.G. Croissant, X. Cattoën, J.-O. Durand, M. Wong Chi Man, N.M. Khashab, Organosilica hybrid nanomaterials with a high organic content: syntheses and applications of silsesquioxanes, Nanoscale 8 (2016) 19945–19972, https://doi.org/10.1039/C6NR06862F.
[188] I. Roy, T.Y. Ohulchanskyy, H.E. Pudavar, E.J. Bergey, A.R. Oseroff, J. Morgan, et al., Ceramic-based nanoparticles entrapping water-insoluble photosensitizing anticancer drugs: a novel drug-carrier system for photodynamic therapy, J. Am. Chem. Soc. 125 (2003) 7860–7865, https://doi.org/10.1021/ja0343095.
[189] F. Barandeh, P.-L. Nguyen, R. Kumar, G.J. Iacobucci, M.L. Kuznicki, A. Kosterman, et al., Organically modified silica nanoparticles are biocompatible and can be targeted to neurons in vivo, PLoS One 7 (2012) e29424, https://doi.org/10.1371/journal.pone.0029424.
[190] Y. Fatieiev, J.G. Croissant, K. Julfakyan, L. Deng, D.H. Anjum, A. Gurinov, et al., Enzymatically degradable hybrid organic–inorganic bridged silsesquioxane nanoparticles for in vitro imaging, Nanoscale 7 (2015) 15046–15050, https://doi.org/10.1039/C5NR03065J.
[191] J.G. Croissant, C. Mauriello-Jimenez, M. Maynadier, X. Cattoën, M. Wong Chi Man, L. Raehm, et al., Synthesis of disulfide-based biodegradable bridged silsesquioxane nanoparticles for two-photon imaging and therapy of cancer cells, Chem. Commun. 51 (2015) 12324–12327, https://doi.org/10.1039/C5CC03736K.
[192] K. Hayashi, M. Nakamura, H. Miki, S. Ozaki, M. Abe, T. Matsumoto, et al., Photostable iodinated silica/porphyrin hybrid nanoparticles with heavy-atom effect for wide-field photodynamic/photothermal therapy using single light source, Adv. Funct. Mater. 24 (2014) 503–513, https://doi.org/10.1002/adfm.201301771.
[193] H. Wang, Y. Liu, M. Li, H. Huang, H.M. Xu, R.J. Hong, et al., Multifunctional TiO2 nanowires-modified nanoparticles bilayer film for 3D dye-sensitized solar cells, Optoelectron. Adv. Mater. Rapid Commun. 4 (2010) 1166–1169, https://doi.org/10.1039/b000000x.
[194] J. Croissant, X. Cattoën, M.W.C. Man, A. Gallud, L. Raehm, P. Trens, et al., Biodegradable ethylene-bis(propyl)disulfide-based periodic mesoporous organosilica nanorods and nanospheres for efficient in-vitro drug delivery, Adv. Mater. 26 (2014) 6174–6180, https://doi.org/10.1002/adma.201401931.
[195] Y. Fatieiev, J.G. Croissant, K. Alamoudi, N.M. Khashab, Cellular internalization and biocompatibility of periodic mesoporous organosilica nanoparticles with tunable morphologies: from nanospheres to nanowires, Chempluschem 82 (2017) 631–637, https://doi.org/10.1002/cplu.201600560.
[196] C. Urata, H. Yamada, R. Wakabayashi, Y. Aoyama, S. Hirosawa, S. Arai, et al., Aqueous colloidal mesoporous nanoparticles with ethenylene-bridged silsesquioxane frameworks, J. Am. Chem. Soc. 133 (2011) 8102–8105, https://doi.org/10.1021/ja201779d.
[197] T. Nash, A.C. Allison, J.S. Harington, K.B. Olsen, E.A. Lepel, J.C. Laul, et al., Physico-chemical properties of silica in relation to its toxicity, Nature 210 (1966) 259–261, https://doi.org/10.1021/AC60052A021.
[198] Slowing, et al., Mesoporous silica nanoparticles for reducing hemolytic activity towards mammalian red blood cells, Small 5 (2009) 57–62, https://doi.org/10.1002/smll.200800926.
[199] Y. Chen, P. Xu, H. Chen, Y. Li, W. Bu, Z. Shu, et al., Colloidal HPMO nanoparticles: silica-etching chemistry tailoring, topological transformation, and nano-biomedical applications, Adv. Mater. 25 (2013) 3100–3105, https://doi.org/10.1002/adma.201204685.
[200] Z. Teng, J. Zhang, W. Li, Y. Zheng, X. Su, Y. Tang, et al., Facile synthesis of yolk–shell-structured triple-hybridized periodic mesoporous organosilica nanoparticles for biomedicine, Small (2016) 3550–3558, https://doi.org/10.1002/smll.201600616.
[201] Q. He, J. Zhang, J. Shi, Z. Zhu, L. Zhang, W. Bu, et al., The effect of PEGylation of mesoporous silica nanoparticles on nonspecific binding of serum proteins and cellular responses, Biomaterials 31 (2010) 1085–1092, https://doi.org/10.1016/j.biomaterials.2009.10.046.
[202] Y.-S. Lin, N. Abadeer, C.L. Haynes, Stability of small mesoporous silicananoparticles in biological media, Chem. Commun. 47 (2011) 532–534, https://doi.org/10.1039/C0CC02923H.
[203] J.L. Townson, Y.S. Lin, J.O. Agola, E.C. Carnes, H.S. Leong, J.D. Lewis, et al., Re-examining the size/charge paradigm: differing in vivo characteristics of size- and charge-matched mesoporous silica nanoparticles, J. Am. Chem. Soc. 135 (2013) 16030–16033, https://doi.org/10.1021/ja4082414.
[204] A. Noureddine, M. Gary-Bobo, L. Lichon, M. Garcia, J.I. Zink, M. Wong Chi Man, et al., Bis-clickable mesoporous silica nanoparticles: straightforward preparation of light-actuated nanomachines for controlled drug delivery with active targeting, Chem. Eur. J. 22 (2016) 9624–9630, https://doi.org/10.1002/chem.201600870.
[205] S. Salmaso, P. Caliceti, Stealth properties to improve therapeutic efficacy of drug nanocarriers, J. Drug Deliv. 2013 (2013) 1–19, https://doi.org/10.1155/2013/374252.
[206] W. Liu, A. Chaix, M. Gary-Bobo, B. Angeletti, A. Masion, A. Da Silva, et al., Stealth biocompatible si-based nanoparticles for biomedical applications, Nanomaterials 7 (2017) 288, https://doi.org/10.3390/nano7100288.
[207] M.R. Mohammadi, A. Nojoomi, M. Mozafari, A. Dubnika, M. Inayathullah, J. Rajadas, Nanomaterials engineering for drug delivery: a hybridization approach, J. Mater. Chem. B 5 (2017) 3995–4018, https://doi.org/10.1039/C6TB03247H.
[208] M. Arruebo, R. Fernández-Pacheco, M.R. Ibarra, J. Santamaría, Magnetic nanoparticles for drug delivery, Nano Today 2 (2007) 22–32, https://doi.org/10.1016/S1748-0132(07)70084-1.
[209] I. Roy, T.Y. Ohulchanskyy, D.J. Bharali, H.E. Pudavar, R.A. Mistretta, N. Kaur, et al., Optical tracking of organically modified silica nanoparticles as DNA carriers: a nonviral, nanomedicine approach for gene delivery, Proc. Natl. Acad. Sci. 102 (2005) 279–284, https://doi.org/10.1073/pnas.0408039101.
[210] D.J. Bharali, I. Klejbor, E.K. Stachowiak, P. Dutta, I. Roy, N. Kaur, et al., Organically modified silica nanoparticles: a nonviral vector for in vivo gene delivery and expression in the brain, Proc. Natl. Acad. Sci. U.S.A. 102 (2005) 11539–11544, https://doi.org/10.1073/pnas.0504926102.
[211] L. Fertier, C. Théron, C. Carcel, P. Trens, M. Wong Chi Man, PH-responsive bridged silsesquioxane, Chem. Mater. 23 (2011) 2100–2106, https://doi.org/10.1021/cm103327y.
[212] S. Giret, C. Théron, A. Gallud, M. Maynadier, M. Gary-Bobo, M. Garcia, et al., A designed 5-fluorouracil-based bridged silsesquioxane as an autonomous acid-triggered drug-delivery system, Chem. Eur. J. 19 (2013) 12806–12814, https://doi.org/10.1002/chem.201301081.
[213] N. Koike, T. Ikuno, T. Okubo, A. Shimojima, Synthesis of monodisperse organosilica nanoparticles with hollow interiors and porous shells using silica nanospheres as templates, Chem. Commun. 49 (2013) 4998, https://doi.org/10.1039/c3cc41904e.
[214] R.P. Singh, S. Dhanalakshmi, C. Agarwal, R. Agarwal, Silibinin strongly inhibits growth and survival of human endothelial cells via cell cycle arrest and downregulation of survivin, Akt and NF-kappaB: implications for angioprevention and antiangiogenic therapy, Oncogene 24 (2005) 1188–1202, https://doi.org/10.1038/sj.onc.1208276.
[215] M. Wu, Y. Chen, L. Zhang, X. Li, X. Cai, Y. Du, et al., A salt-assisted acid etching strategy for hollow mesoporous silica/organosilica for pH-responsive drug and gene co-delivery, J. Mater. Chem. B 3 (2015) 766–775, https://doi.org/10.1039/C4TB01581A.
[216] Y. Gao, Y. Chen, X. Ji, X. He, Q. Yin, Z. Zhang, et al., Controlled intracellular release of doxorubicin in multidrug-resistant cancer cells by tuning the shell-pore sizes of mesoporous silica nanoparticles, ACS Nano 5 (2011) 9788–9798, https://doi.org/10.1021/nn2033105.
[217] M. Kim, H. Na, Y. Kim, S. Ryoo, H.S. Cho, K.E. Lee, et al., Facile synthesis of monodispersed mesoporous silica nanoparticles with ultralarge pores and their application in gene delivery, ACS Nano (2011) 3568–3576, https://doi.org/10.1021/nn103130q.
[218] S.B. Hartono, W. Gu, F. Kleitz, J. Liu, L. He, A.P.J. Middelberg, et al., Poly-L-lysine functionalized large pore cubic mesostructured silica nanoparticles as biocompatible carriers for gene delivery, ACS Nano 6 (2012) 2104–2117, https://doi.org/10.1021/nn2039643.
[219] H.K. Na, M.H. Kim, K. Park, S.R. Ryoo, K.E. Lee, H. Jeon, et al., Efficient functional delivery of siRNA using mesoporous silica nanoparticles with ultralarge pores, Small 8 (2012) 1752–1761, https://doi.org/10.1002/smll.201200028.
[220] Y. Li, M. Kruk, Single-micelle-templated synthesis of hollow silica nanospheres with tunable pore structures, RSC Adv. 5 (2015) 69870–69877, https://doi.org/10.1039/C5RA13492G.
[221] N.Ž. Knežević, J.-O. Durand, Large pore mesoporous silica nanomaterials for application in delivery of biomolecules, Nanoscale 7 (2015) 2199–2209, https://doi.org/10.1039/C4NR06114D.
[222] Y. Han, J.Y. Ying, Generalized fluorocarbon-surfactant-mediated synthesis of nanoparticles with various mesoporous structures, Angew. Chem. Int. Ed. 44 (2004) 288–292, https://doi.org/10.1002/anie.200460892.
[223] J. Sun, H. Zhang, R. Tian, D. Ma, X. Bao, D.S. Su, et al., Ultrafast enzyme immobilization over large-pore nanoscale mesoporous silica particles, Chem. Commun. 1 (2006) 1322, https://doi.org/10.1039/b516930e.
[224] F. Gao, P. Botella, A. Corma, J. Blesa, L. Dong, Monodispersed mesoporous silica nanoparticles with very large pores for enhanced adsorption and release of DNA, J. Phys. Chem. B 113 (2009) 1796–1804, https://doi.org/10.1021/jp807956r.
[225] I.I. Slowing, B.G. Trewyn, V.S.Y. Lin, Mesoporous silica nanoparticles for intracellular delivery of membrane-impermeable proteins, J. Am. Chem. Soc. 129 (2007) 8845–8849, https://doi.org/10.1021/ja0719780.

[226] M. Kruk, Access to ultralarge-pore ordered mesoporous materials through selection of surfactant/swelling-agent micellar templates, Acc. Chem. Res. 45 (2012).
[227] C. Tao, Y. Zhu, Y. Xu, M. Zhu, H. Morita, N. Hanagata, Mesoporous silica nanoparticles for enhancing the delivery efficiency of immunostimulatory DNA drugs, Dalton Trans. 43 (2014) 5142–5150, https://doi.org/10.1039/c3dt53433b.
[228] D.H. Han, H.-K. Na, W.H. Choi, J.H. Lee, Y.K. Kim, C. Won, et al., Direct cellular delivery of human proteasomes to delay tau aggregation, Nat. Commun. 5 (2014) 5633, https://doi.org/10.1038/ncomms6633.
[229] C.Y. Lai, B.G. Trewyn, D.M. Jeftinija, K. Jeftinija, S. Xu, S. Jeftinija, et al., A mesoporous silica nanosphere-based carrier system with chemically removable CdS nanoparticle caps for stimuli-responsive controlled release of neurotransmitters and drug molecules, J. Am. Chem. Soc. 125 (2003) 4451–4459, https://doi.org/10.1021/ja028650l.
[230] K. Zhang, L.L. Xu, J.G. Jiang, N. Calin, K.F. Lam, S.J. Zhang, et al., Facile large-scale synthesis of monodisperse mesoporous silica nanospheres with tunable pore structure, J. Am. Chem. Soc. 135 (2013) 2427–2430, https://doi.org/10.1021/ja3116873.
[231] Y. Yang, Y. Niu, J. Zhang, A.K. Meka, H. Zhang, C. Xu, et al., Biphasic synthesis of large-pore and well-dispersed benzene bridged mesoporous organosilica nanoparticles for intracellular protein delivery, Small 11 (2015) 2743–2749, https://doi.org/10.1002/smll.201402779.
[232] T. Kubota, T. Iwai, K. Sakai, T. Gonoi, J. Kobayashi, Optical identification of single- and few-layer MoS2 sheets [supporting information], Org. Lett. 16 (2014) 5624–5627, https://doi.org/10.1002/smll.
[233] V.J. Yao, S. D'Angelo, K.S. Butler, C. Theron, T.L. Smith, S. Marchiò, et al., Ligand-targeted theranostic nanomedicines against cancer, J. Control. Release 240 (2016) 267–286, https://doi.org/10.1016/j.jconrel.2016.01.002.
[234] S. Giri, B.G. Trewyn, M.P. Stellmaker, V.S.Y. Lin, Stimuli-responsive controlled-release delivery system based on mesoporous silica nanorods capped with magnetic nanoparticles, Angew. Chem. Int. Ed. 44 (2005) 5038–5044, https://doi.org/10.1002/anie.200501819.
[235] R. Mortera, J. Vivero-Escoto, I.I. Slowing, E. Garrone, B. Onida, V.S.-Y. Lin, Cell-induced intracellular controlled release of membrane impermeable cysteine from a mesoporous silica nanoparticle-based drug delivery system, Chem. Commun. 36 (2009) 3219, https://doi.org/10.1039/b900559e.
[236] V.S.Y. Lin, C.Y. Lai, J. Huang, S.A. Song, S. Xu, Molecular recognition inside of multifunctionalized mesoporous silicas: toward selective fluorescence detection of dopamine and glucosamine [8], J. Am. Chem. Soc. 123 (2001) 11510–11511, https://doi.org/10.1021/ja016223m.
[237] A. Baeza, R.R. Castillo, A. Torres-Pardo, J.M. González-Calbet, M. Vallet-Regí, Electron microscopy for inorganic-type drug delivery nanocarriers for antitumoral applications: what does it reveal?, J. Mater. Chem. B 5 (2017) 2714–2725, https://doi.org/10.1039/C6TB03062A.
[238] M. Vallet-Regí, E. Ruiz-Hernández, Bioceramics: from bone regeneration to cancer nanomedicine, Adv. Mater. 23 (2011) 5177–5218, https://doi.org/10.1002/adma.201101586.
[239] M. Vallet-Regí, M. Colilla, B. González, Medical applications of organic–inorganic hybrid materials within the field of silica-based bioceramics, Chem. Soc. Rev. 40 (2011) 596–607, https://doi.org/10.1039/C0CS00025F.
[240] P. Horcajada, A. Rámila, J. Pérez-Pariente, M. Vallet-Regí, Influence of pore size of MCM-41 matrices on drug delivery rate, Microporous Mesoporous Mater. 68 (2004) 105–109, https://doi.org/10.1016/j.micromeso.2003.12.012.
[241] S. Quignard, S. Masse, G. Laurent, T. Coradin, Introduction of disulfide bridges within silica nanoparticles to control their intra-cellular degradation, Chem. Commun. 49 (2013) 3410, https://doi.org/10.1039/c3cc41062e.
[242] J.G. Croissant, Y. Fatieiev, N.M. Khashab, Degradability and clearance of silicon, organosilica, silsesquioxane, silica mixed oxide, and mesoporous silica nanoparticles, Adv. Mater. 29 (2017) https://doi.org/10.1002/adma.201604634.
[243] S. Datz, H. Engelke, C.V. Schirnding, L. Nguyen, T. Bein, Lipid bilayer-coated curcumin-based mesoporous organosilica nanoparticles for cellular delivery, Microporous Mesoporous Mater. 225 (2016) 371–377, https://doi.org/10.1016/j.micromeso.2015.12.006.
[244] L. Maggini, I. Cabrera, A. Ruiz-Carretero, E.A. Prasetyanto, E. Robinet, L. De Cola, Breakable mesoporous silica nanoparticles for targeted drug delivery, Nanoscale 8 (2016) 7240–7247, https://doi.org/10.1039/C5NR09112H.
[245] Q. Zhang, C. Shen, N. Zhao, F.J. Xu, Redox-responsive and drug-embedded silica nanoparticles with unique self-destruction features for efficient gene/drug codelivery, Adv. Funct. Mater. 27 (2017) 1–12, https://doi.org/10.1002/adfm.201606229.
[246] J.G. Croissant, Y. Fatieiev, K. Julfakyan, J. Lu, A.H. Emwas, D.H. Anjum, et al., Biodegradable oxamide-phenylene-based mesoporous organosilica nanoparticles with unprecedented drug payloads for delivery in cells, Chem. Eur. J. 22 (2016) 14806–14811, https://doi.org/10.1002/chem.201601714.
[247] J. Della Rocca, M.E. Werner, S.A. Kramer, R.C. Huxford-Phillips, R. Sukumar, N.D. Cummings, et al., Polysilsesquioxane nanoparticles for triggered release of cisplatin and effective cancer chemoradiotherapy, Nanomed. Nanotechnol. Biol. Med. 11 (2015) 31–38, https://doi.org/10.1016/j.nano.2014.07.004.
[248] J. Della Rocca, R.C. Huxford, E. Comstock-Duggan, W. Lin, Polysilsesquioxane nanoparticles for targeted platin-based cancer chemotherapy by triggered release, Angew. Chem. Int. Ed. 50 (2011) 10330–10334, https://doi.org/10.1002/anie.201104510.
[249] J.L. Vivero-Escoto, W.J. Rieter, H. Lau, R.C. Huxford-Phillips, W. Lin, Biodegradable polysilsesquioxane nanoparticles as efficient contrast agents for magnetic resonance imaging, Small 9 (2013) 3523–3531, https://doi.org/10.1002/smll.201300198.
[250] M.H. Lee, Z. Yang, C.W. Lim, Y.H. Lee, S. Dongbang, C. Kang, et al., Disulfide-cleavage-triggered chemosensors and their biological applications, Chem. Rev. 113 (2013) 5071–5109, https://doi.org/10.1021/cr300358b.
[251] L.C. Hu, Y. Yonamine, S.H. Lee, W.E. Van Der Veer, K.J. Shea, Light-triggered charge reversal of organic-silica hybrid nanoparticles, J. Am. Chem. Soc. 134 (2012) 11072–11075, https://doi.org/10.1021/ja303118w.
[252] Y. Hoshino, H. Koide, K. Furuya, W.W. Haberaecker, S.-H. Lee, T. Kodama, et al., The rational design of a synthetic polymer nanoparticle that neutralizes a toxic peptide in vivo, Proc. Natl. Acad. Sci. 109 (2012) 33–38, https://doi.org/10.1073/pnas.1112828109.
[253] Y. Hoshino, H. Koide, T. Urakami, H. Kanazawa, T. Kodama, N. Oku, et al., Recognition, neutralization and clearance of target peptides in the blood stream of living mice by molecular imprinted polymer nanoparticles: a plastic antibody, J. Am. Chem. Soc. (2010) 1–5, https://doi.org/10.1021/ja102148f.
[254] Y. Fatieiev, J.G. Croissant, S. Alsaiari, B.A. Moosa, D.H. Anjum, N.M. Khashab, Photoresponsive bridged silsesquioxane nanoparticles with tunable morphology for light-triggered plasmid DNA delivery, ACS Appl. Mater. Interfaces 7 (2015) 24993–24997, https://doi.org/10.1021/acsami.5b07365.
[255] A.P. Blum, J.K. Kammeyer, A.M. Rush, C.E. Callmann, M.E. Hahn, N.C. Gianneschi, Stimuli-responsive nanomaterials for biomedical applications, J. Am. Chem. Soc. 137 (2015) 2140–2154, https://doi.org/10.1021/ja510147n.
[256] J. Dong, J.I. Zink, Light or heat? The origin of cargo release from nanoimpeller particles containing upconversion nanocrystals under IR irradiation, Small 11 (2015) 4165–4172, https://doi.org/10.1002/smll.201500607.
[257] D. Tarn, M. Xue, J.I. Zink, PH-responsive dual cargo delivery from mesoporous silica nanoparticles with a metal-latched nanogate, Inorg. Chem. 52 (2013) 2044–2049, https://doi.org/10.1021/ic3024265.
[258] A. Schlossbauer, S. Warncke, P.M.E. Gramlich, J. Kecht, A. Manetto, T. Carell, et al., A programmable DNA-based molecular valve for colloidal mesoporous silica, Angew. Chem. Int. Ed. 49 (2010) 4734–4737, https://doi.org/10.1002/anie.201000827.
[259] V. Cauda, A. Schlossbauer, J. Kecht, A. Zürner, T. Bein, Multiple core-shell functionalized colloidal mesoporous silica nanoparticles, J. Am. Chem. Soc. 131 (2009) 11361–11370, https://doi.org/10.1021/ja809346n.
[260] M. Martínez-Carmona, A. Baeza, M.A. Rodriguez-Milla, J. García-Castro, M. Vallet-Regí, Mesoporous silica nanoparticles grafted with a light-responsive protein shell for highly cytotoxic antitumoral therapy, J. Mater. Chem. B 3 (2015) 5746–5752, https://doi.org/10.1039/C5TB00304K.
[261] A. Baeza, M. Colilla, M. Vallet-Regí, Advances in mesoporous silica nanoparticles for targeted stimuli-responsive drug delivery, Exp. Opin. Drug Deliv. 12 (2015) 319–337, https://doi.org/10.1517/17425247.2014.953051.
[262] A. Baeza, E. Guisasola, E. Ruiz-Hernández, M. Vallet-Regí, Magnetically triggered multidrug release by hybrid mesoporous silica nanoparticles, Chem. Mater. 24 (2012) 517–524, https://doi.org/10.1021/cm203000u.
[263] M. Colilla, A. Baeza, M. Vallet-Regí, Mesoporous silica nanoparticles for drug delivery and controlled release applications, in: Handb. Sol Gel Chem., 2015. doi: 10.1002/9783527670819.ch42.
[264] K.K. Cotí, M.E. Belowich, M. Liong, M.W. Ambrogio, Y.A. Lau, H.A. Khatib, et al., Mechanised nanoparticles for drug delivery, Nanoscale 1 (2009) 16, https://doi.org/10.1039/b9nr00162j.
[265] T.M. Guardado-Alvarez, L. Sudha Devi, M.M. Russell, B.J. Schwartz, J.I. Zink, Activation of snap-top capped mesoporous silica nanocontainers using two near-infrared photons, J. Am. Chem. Soc. 135 (2013) 14000–14003, https://doi.org/10.1021/ja407331n.
[266] S. Angelos, E. Choi, F. Vögtle, L. De Cola, J.I. Zink, Photo-driven expulsion of molecules from mesostructured silica nanoparticles, J. Phys. Chem. C 111 (2007) 6589–6592, https://doi.org/10.1021/jp0707211.
[267] X. Li, L. Zhou, Y. Wei, A.M. El-Toni, F. Zhang, D. Zhao, Anisotropic growth-induced synthesis of dual-compartment janus mesoporous silica nanoparticles for bimodal triggered drugs delivery, J. Am. Chem. Soc. 136 (2014) 15086–15092, https://doi.org/10.1021/ja508733r.
[268] N. Liu, Z. Chen, D.R. Dunphy, Y.B. Jiang, R.A. Assink, C.J. Brinker, Photoresponsive nanocomposite formed by self-assembly of an azobenzene-modified silane, Angew. Chem. Int. Ed. 42 (2003) 1731–1734, https://doi.org/10.1002/anie.200250189.
[269] E. Choi, J. Lu, F. Tamanoi, J.I. Zink, Drug release from three-dimensional cubic Mesoporous silica nanoparticles controlled by nanoimpellers, Zeitschrift Fur Anorg. Und Allg. Chem. 640 (2014) 588–594, https://doi.org/10.1002/zaac.201300503.
[270] H.M.D. Bandara, S.C. Burdette, Photoisomerization in different classes of azobenzene, Chem. Soc. Rev. 41 (2012) 1809–1825, https://doi.org/10.1039/C1CS15179G.
[271] J. Croissant, M. Maynadier, A. Gallud, H. Peindy N'Dongo, J.L. Nyalosaso, G. Derrien, et al., Two-photon-triggered drug delivery in cancer cells using nanoimpellers, Angew. Chem. Int. Ed. 52 (2013) 13813–13817, https://doi.org/10.1002/anie.201308647.
[272] X. Li, L. Zhou, Y. Wei, A.M. El-Toni, F. Zhang, D. Zhao, Anisotropic encapsulation-induced synthesis of asymmetric single-hole mesoporous nanocages, J. Am. Chem. Soc. 137 (2015) 5903–5906, https://doi.org/10.1021/jacs.5b03207.
[273] J. Croissant, D. Salles, M. Maynadier, O. Mongin, V. Hugues, M. Blanchard-desce, et al., Mixed periodic mesoporous organosilica nanoparticles and core – shell systems, application to in vitro two-photon imaging, therapy, and drug delivery, Chem. Mater. 26 (2014) 7214–7220.
[274] X. Cattoën, A. Noureddine, J. Croissant, N. Moitra, K. Bürglová, J. Hodačová, et al., Click approaches in sol-gel chemistry, J. Sol-Gel Sci. Technol. 70 (2014) 245–253, https://doi.org/10.1007/s10971-013-3155-x.
[275] O. De Los Cobos, B. Fousseret, M. Lejeune, F. Rossignol, M. Dutreilh-Colas, C. Carrion, et al., Tunable multifunctional mesoporous silica microdots arrays by combination of inkjet printing, eisa, and click chemistry, Chem. Mater. 24 (2012) 4337–4342, https://doi.org/10.1021/cm3022769.

[276] N. Moitra, J.J.E. Moreau, X. Cattoen, M. Wong Chi Man, Convenient route to water-sensitive sol-gel precursors using click chemistry, Chem. Commun. 46 (2010) 8416–8418, https://doi.org/10.1039/C0CC03417G.
[277] K. Bürglová, N. Moitra, J. Hodačová, X. Cattoën, M. Wong Chi Man, Click approaches to functional water-sensitive organotriethoxysilanes, J. Org. Chem. 76 (2011) 7326–7333, https://doi.org/10.1021/jo201484n.
[278] V.D. Bock, H. Hiemstra, J.H. Van Maarseveen, Cu I-catalyzed alkyne-azide "click" cycloadditions from a mechanistic and synthetic perspective, Eur. J. Org. Chem. 40 (2006) 51–68, https://doi.org/10.1002/ejoc.200500483.
[279] N. Moitra, P. Trens, L. Raehm, J.-O. Durand, X. Cattoën, M.W. Chi Man, Facile route to functionalized mesoporous silica nanoparticles by click chemistry, J. Mater. Chem. 21 (2011) 13476, https://doi.org/10.1039/c1jm12066b.
[280] J. Nakazawa, T.D.P. Stack, Controlled loadings in a mesoporous material: click-on silica, J. Am. Chem. Soc. 130 (2008) 14360–14361, https://doi.org/10.1021/ja804237b.
[281] B. Malvi, B.R. Sarkar, D. Pati, R. Mathew, T.G. Ajithkumar, S. Sen Gupta, "Clickable" SBA-15 mesoporous materials: synthesis, characterization and their reaction with alkynes, 1409 J. Mater. Chem. 19 (2009) https://doi.org/10.1039/b815350g.
[282] A. Schlossbauer, D. Schaffert, J. Kecht, E. Wagner, T. Bein, Click chemistry for high-density biofunctionalization of mesoporous silica, J. Am. Chem. Soc. 130 (2008) 12558–12559, https://doi.org/10.1021/ja803018w.
[283] M. Meldal, C.W. Tomøe, Cu-catalyzed azide – alkyne cycloaddition, Chem. Rev. 108 (2008) 2952–3015, https://doi.org/10.1021/cr0783479.
[284] S. Shenoi-Perdoor, A. Noureddine, F. Dubois, M. Wong Chi Man, X. Cattoën, Click functionalization of sol-gel materials, in: Handb. Sol Gel Chem., 2016.
[285] C. Mauriello-Jimenez, J. Croissant, M. Maynadier, X. Cattoën, M. Wong Chi Man, J. Vergnaud, et al., Porphyrin-functionalized mesoporous organosilica nanoparticles for two-photon imaging of cancer cells and drug delivery, J. Mater. Chem. B 3 (2015) 3681–3684, https://doi.org/10.1039/C5TB00315F.
[286] UCLA, Ucla Health, Web. (2014).
[287] H. Tang, Y. Zheng, Y. Chen, Materials chemistry of nanoultrasonic biomedicine, Adv. Mater. 29 (2017) https://doi.org/10.1002/adma.201604105.
[288] X. Wang, H. Chen, K. Zhang, M. Ma, F. Li, D. Zeng, et al., An intelligent nanotheranostic agent for targeting, redox-responsive ultrasound imaging, and imaging-guided high-intensity focused ultrasound synergistic therapy, Small 10 (2014) 1403–1411, https://doi.org/10.1002/smll.201302846.
[289] Y. Li, R. Tong, H. Xia, H. Zhang, J. Xuan, High intensity focused ultrasound and redox dual responsive polymer micelles, Chem. Commun. 46 (2010) 7739–7741, https://doi.org/10.1039/c0cc02628j.
[290] X. Wang, H. Chen, Y. Chen, M. Ma, K. Zhang, F. Li, et al., Perfluorohexane-encapsulated mesoporous silica nanocapsules as enhancement agents for highly efficient high intensity focused ultrasound (HIFU), Adv. Mater. 24 (2012) 785–791, https://doi.org/10.1002/adma.201104033.
[291] X. Qian, W. Wang, W. Kong, Y. Chen, Organic-inorganic hybrid hollow mesoporous organosilica nanoparticles for efficient ultrasound-based imaging and controlled drug release, J. Nanomater. 2014 (2014).
[292] X. Qian, W. Wang, W. Kong, Y. Chen, Hollow periodic mesoporous organosilicas for highly efficient HIFU-based synergistic therapy, RSC Adv. 4 (2014) 17950–17958, https://doi.org/10.1039/C3RA47654E.
[293] C.J. Brinker, Nanoparticle immunotherapy: combo combat, Nat. Mater. 11 (2012) 831–832, https://doi.org/10.1038/nmat3434.
[294] J. Park, S.H. Wrzesinski, E. Stern, M. Look, J. Criscione, R. Ragheb, et al., Combination delivery of TGF-β inhibitor and IL-2 by nanoscale liposomal polymeric gels enhances tumour immunotherapy, Nat. Mater. 11 (2012) 895–905, https://doi.org/10.1038/nmat3355.

Achraf Noureddine earned his PhD in materials chemistry from the Chemical Engineering School of Montpellier (ENSCM-France, 2014) with Prof. Michel Wong Chi Man and Prof. Xavier Cattoën. He then joined the European Center of Ceramics as a postdoctoral fellow to work on ink-jet printed silica materials with Prof. Martine Lejeune and Prof. Fabrice Rossignol. In 2016, he joined Prof. Jeffrey Brinker's lab at the University of New Mexico as a postdoctoral associate to develop new porous silica and organosilica nanoparticles-supported lipid bilayer (*aka* Protocells) for advanced biomedical applications.

Jeff Brinker is currently one of three Sandia National Laboratory Fellows and Distinguished and Regent's Professor of Chemical and Biological Engineering, Molecular Genetics and Microbiology and member of the Comprehensive Cancer Center at the University of New Mexico. He is Co-Director of the UNM Center for Micro-Engineered Materials. Brinker is recognized for his pioneering efforts in sol–gel processing and its combination with molecular self-assembly in a process referred to as evaporation-induced self-assembly, enabling the formation of highly ordered mesoporous films and particles. He also invented mesoporous silica nanoparticle supported lipid bilayers aka *protocells* as a new universal drug delivery vehicle.